Conifers, Angiosperm Trees, and Lianas: Growth, Whole-Plant Water and Nitrogen Use Efficiency, and Stable Isotope Composition ($\delta^{13}C$ and $\delta^{18}O$) of Seedlings Grown in a Tropical Environment[1][W][OA]

Lucas A. Cernusak[2]*, Klaus Winter, Jorge Aranda, and Benjamin L. Turner

Smithsonian Tropical Research Institute, Balboa, Ancon, Republic of Panama

Seedlings of several species of gymnosperm trees, angiosperm trees, and angiosperm lianas were grown under tropical field conditions in the Republic of Panama; physiological processes controlling plant C and water fluxes were assessed across this functionally diverse range of species. Relative growth rate, *r*, was primarily controlled by the ratio of leaf area to plant mass, of which specific leaf area was a key component. Instantaneous photosynthesis, when expressed on a leaf-mass basis, explained 69% of variation in *r* ($P < 0.0001$, $n = 94$). Mean *r* of angiosperms was significantly higher than that of the gymnosperms; within angiosperms, mean *r* of lianas was higher than that of trees. Whole-plant nitrogen use efficiency was also significantly higher in angiosperm than in gymnosperm species, and was primarily controlled by the rate of photosynthesis for a given amount of leaf nitrogen. Whole-plant water use efficiency, TE_c, varied significantly among species, and was primarily controlled by c_i/c_a, the ratio of intercellular to ambient CO_2 partial pressures during photosynthesis. Instantaneous measurements of c_i/c_a explained 51% of variation in TE_c ($P < 0.0001$, $n = 94$). Whole-plant ^{13}C discrimination also varied significantly as a function of c_i/c_a ($R^2 = 0.57$, $P < 0.0001$, $n = 94$), and was, accordingly, a good predictor of TE_c. The ^{18}O enrichment of stem dry matter was primarily controlled by the predicted ^{18}O enrichment of evaporative sites within leaves ($R^2 = 0.61$, $P < 0.0001$, $n = 94$), with some residual variation explained by mean transpiration rate. Measurements of carbon and oxygen stable isotope ratios could provide a useful means of parameterizing physiological models of tropical forest trees.

Tropical forest ecosystems have been subject to extensive perturbations associated with anthropogenic activity in recent decades, and such perturbations will likely continue into the foreseeable future (Laurance et al., 2004; Wright, 2005). Effective environmental management requires knowledge of how such perturbations impact upon cycling of carbon (C) and water between forest trees and the atmosphere, and how these C and water fluxes relate to plant nutrient status. A sound, mechanistic understanding of the physiological processes that control photosynthesis and transpiration in tropical trees is therefore essential for understanding and managing the human impact upon tropical forests. In this study, we analyzed the physiological controls over growth (the relative rate of C accumulation), nitrogen (N) use efficiency (NUE; the rate of C accumulation for a given N content), water use efficiency (the ratio of whole-plant C gain to water loss), and stable isotope composition ($\delta^{13}C$ and $\delta^{18}O$) in seedlings of a diverse suite of species grown side-by-side in a tropical environment.

Conifers dominated the world's forests prior to the Cretaceous radiation in angiosperm diversity. However, conifers are largely absent from the lowland tropical and subtropical forests of today. It has been suggested that one means by which angiosperm tree species are able to out-compete gymnosperm tree species in tropical environments is through faster seedling growth caused by improved hydraulic efficiency (Bond, 1989; Brodribb et al., 2005). Angiosperm xylem tissue contains vessels, specialized water-conducting cells that are generally larger in diameter, and therefore more conductive to water, than conifer tracheids (Sperry et al., 2006). Conifer tracheid diameters are biomechanically constrained because these cells must perform the dual function of conducting water and providing structural support to woody tissues, whereas vessels need not perform the latter function in angiosperm wood. Lianas are large woody vines that occur predominantly in tropical forests; by attaching themselves to neighboring trees, they have evolved an additional means of freeing their xylem tissues from structural constraints. Thus, angiosperm lianas may achieve further increases in hydraulic efficiency compared to angiosperm trees (Gartner et al., 1990).

[1] This work was supported by the Smithsonian Tropical Research Institute. L.A.C. was supported by a postdoctoral fellowship from the Smithsonian Institution and a Tupper Research Fellowship from the Smithsonian Tropical Research Institute.

[2] Present address: School of Environmental and Life Sciences, Charles Darwin University, Darwin, Northern Territory 0909, Australia.

* Corresponding author; e-mail lucas.cernusak@cdu.edu.au.

The author responsible for distribution of materials integral to the findings presented in this article in accordance with the policy described in the Instructions for Authors (www.plantphysiol.org) is: Lucas A. Cernusak (lucas.cernusak@cdu.edu.au).

[W] The online version of this article contains Web-only data.

[OA] Open Access article can be viewed online without a subscription.

www.plantphysiol.org/cgi/doi/10.1104/pp.108.123521

In this study, we grew seedlings of several species of gymnosperm trees, angiosperm trees, and angiosperm lianas in a tropical environment. We used this functionally diverse range of species to quantify the physiological controls over their C and water fluxes. We also took advantage of the contrasting physiology of the study species to test the theoretical basis for variation in the C and oxygen (O) stable isotope composition of plant dry matter.

THEORY

Growth

Following Masle and Farquhar (1988), and based on earlier treatments (Blackman, 1919; Evans, 1972), we write the following expression to describe factors that influence the relative rate of C accumulation of a plant:

$$r = \frac{1}{m_c} \cdot \frac{dm_c}{dt} = \frac{Al(1 - \phi_c)}{\rho} \quad (1)$$

where r is relative growth rate (mol C mol^{-1} C s^{-1}), m_c is plant C mass (mol C), t is time (s), A is leaf photosynthetic rate (mol C m^{-2} s^{-1}), l is the light period as a fraction of 24 h, ϕ_c is the proportion of C gained in photosynthesis that is subsequently used for respiration by leaves at night and by roots and stems during day and night, and ρ is the ratio of plant C mass to leaf area (mol C m^{-2}). Equation 1 provides a useful tool for examining sources of variation in r among plant species and individuals within a species. It is similar to the classical decomposition of r into net assimilation rate (NAR; g m^{-2} s^{-1}) and leaf area ratio (LAR; m^2 g^{-1}), but allows the assimilation term to be expressed as a net photosynthetic rate, such as would be measured using standard gas exchange techniques (Long et al., 1996). Table I provides definitions of all abbreviations and symbols used in this article.

NUE

Multiplying both sides of Equation 1 by the molar ratio of plant C to N yields an expression for the NUE of C accumulation:

$$\mathrm{NUE} = \frac{1}{m_n} \cdot \frac{dm_c}{dt} = A_n l(1 - \phi_c) n_l \quad (2)$$

where NUE is whole-plant NUE (mol C mol^{-1} N s^{-1}), m_n is plant N mass (mol N), A_n is photosynthetic NUE (mol C mol^{-1} N s^{-1}), and n_l is the proportion of plant N allocated to leaves. Equation 2 provides a basis for linking A_n, a trait often quantified in ecophysiological investigations, with NUE, an integrated measure of NUE at the whole-plant level.

Transpiration Efficiency and C Isotope Discrimination

The ratio of C gain to water loss at the leaf level during photosynthesis can be expressed as the ratio of the diffusive fluxes of CO_2 and water vapor into and out of the leaf, respectively (Farquhar and Richards, 1984):

$$\frac{A}{E} = \frac{c_a - c_i}{1.6\nu} \quad (3)$$

where E is transpiration (mol H_2O m^{-2} s^{-1}), c_a and c_i are CO_2 partial pressures in ambient air and leaf intercellular air spaces, respectively, v is the leaf-to-air vapor pressure difference, and 1.6 is the ratio of diffusivities of CO_2 and H_2O in air. The v is defined as e_i-e_a, where e_i and e_a are the intercellular and ambient vapor pressures, respectively. The ratio of C gain to water loss can be scaled to the whole-plant level by taking into account respiratory C use and water loss not associated with photosynthesis (Farquhar and Richards, 1984; Hubick and Farquhar, 1989):

$$\mathrm{TE_c} = \frac{(1 - \phi_c)c_a\left(1 - \frac{c_i}{c_a}\right)}{1.6\nu(1 + \phi_w)} \quad (4)$$

where $\mathrm{TE_c}$ is the transpiration efficiency of C gain, and ϕ_w is unproductive water loss as a proportion of water loss associated with C uptake, the former mainly comprising water loss at night through partially open stomata. Thus, ϕ_w can be approximated as E_n/E_d, where E_n is nighttime transpiration and E_d is daytime transpiration.

We suggest that the leaf to air vapor pressure difference, v, can be written as the product of the air vapor pressure deficit (D), and a second term, ϕ_v, which describes the magnitude of v relative to D, such that $v = D\phi_v$. This allows Equation 3 to be written as

$$D \cdot \mathrm{TE_c} = \frac{(1 - \phi_c)c_a\left(1 - \frac{c_i}{c_a}\right)}{1.6\phi_v(1 + \phi_w)} \quad (5)$$

Weighting $\mathrm{TE_c}$ by D facilitates comparison of the transpiration efficiency of plants grown under different environmental conditions by accounting for variation due to differences in atmospheric vapor pressure deficit (Tanner and Sinclair, 1983; Hubick and Farquhar, 1989). Thus, it accounts for variation in $\mathrm{TE_c}$ that is purely environmental. The $D{\cdot}\mathrm{TE_c}$ has units of Pa mol C mol^{-1} H_2O.

Photosynthetic discrimination against ^{13}C ($\Delta^{13}C$) shares a common dependence with $\mathrm{TE_c}$ on c_i/c_a. The $\Delta^{13}C$ in C_3 plants relates to c_i/c_a according to the following equation (Farquhar et al., 1982; Farquhar and Richards, 1984; Hubick et al., 1986):

$$\Delta^{13}\mathrm{C} = a - d + (b - a)\frac{c_i}{c_a} \quad (6)$$

where a is the discrimination against ^{13}C during diffusion through stomata (4.4‰), b is discrimination against ^{13}C during carboxylation by Rubisco (29‰), and d is a composite term that summarizes collectively the discriminations associated with dissolution of CO_2,

Table I. *Abbreviations and symbols used in the text*

A	Area-based photosynthesis rate (μmol CO_2 m^{-2} s^{-1})
A_m	Mass-based photosynthesis rate (nmol CO_2 g^{-1} s^{-1})
A_n	Photosynthetic NUE (μmol CO_2 mol^{-1} N s^{-1})
a	Discrimination against ^{13}C during diffusion through stomata
b	Discrimination against ^{13}C during carboxylation by Rubisco
C	Molar concentration of water (mol m^{-3})
c_a	Partial pressure of CO_2 in ambient air (Pa)
c_i	Partial pressure of CO_2 in leaf intercellular air spaces (Pa)
D	Vapor pressure deficit of ambient air (kPa)
D_g	Growth-weighted vapor pressure deficit of ambient air (kPa)
D_i	Average daytime vapor pressure deficit of ambient air during week i (kPa)
D_{18}	Diffusivity of $H_2{}^{18}O$ in water (m^2 s^{-1})
d	Discrimination against ^{13}C during C_3 photosynthesis not associated with a or b
E	Transpiration rate (mmol m^{-2} s^{-1})
E_d	Daytime transpiration rate (mmol m^{-2} s^{-1})
E_t	Cumulative transpiration over the course of the experiment (mol)
E_n	Nighttime transpiration rate (mmol m^{-2} s^{-1})
e_a	Vapor pressure of ambient air (kPa)
e_i	Vapor pressure in leaf intercellular air spaces (kPa)
g_s	Stomatal conductance (mol m^{-2} s^{-1})
L	Scaled effective path length relating to ^{18}O advection and diffusion (m)
LAR	Leaf area ratio (m^2 kg^{-1})
LA_1	Leaf area at the initiation of the experiment (m^2)
LA_2	Leaf area at the conclusion of the experiment (m^2)
l	Light period as a fraction of 24 h
l_c	Mass of C in leaf litter abscised during the experiment (mol C)
m_c	Plant C mass (mol C)
m_{c1}	Plant C mass at the initiation of the experiment (mol C)
m_{c2}	Plant C mass at the conclusion of the experiment (mol C)
m_n	Plant N mass (mol N)
MTR	Mean transpiration rate over the course of the experiment (mol m^{-2} d^{-1})
NAR	Net assimilation rate (g dry matter m^{-2} s^{-1})
NUE	Whole-plant N use efficiency (mol C mol^{-1} N d^{-1})
n_l	Leaf N as a proportion of whole-plant N
P_{area}	Leaf P per unit area (mmol m^{-2})
p_{ex}	Proportion of O atoms exchanging with medium water during cellulose synthesis
p_x	Proportion of water in developing cells not subject to evaporative ^{18}O enrichment
R	The $^{18}O/^{16}O$ ratio of any water or dry matter component of interest
R_a	The $^{13}C/^{12}C$ ratio of CO_2 in ambient air
R_p	The $^{13}C/^{12}C$ ratio of plant C
R_s	The $^{18}O/^{16}O$ ratio of irrigation (source) water
r	Relative growth rate (mol C mol^{-1} C d^{-1})
SLA	Specific leaf area (m^2 kg^{-1})
TE_c	Whole-plant transpiration efficiency of C gain (mmol C mol^{-1} H_2O)
v	Leaf-to-air vapor pressure difference (kPa)
v_g	Growth-weighted leaf-to-air vapor pressure difference (kPa)
v_i	Average daytime leaf-to-air vapor pressure difference for week i (kPa)
w_i	Predicted dry matter increment for week i (g)
$\Delta^{13}C$	Discrimination against ^{13}C
$\Delta^{13}C_p$	Discrimination against ^{13}C in dry matter of the whole plant relative to CO_2 in air
$\Delta^{18}O_e$	The ^{18}O enrichment of evaporative sites within leaves compared to source water
$\Delta^{18}O_{eg}$	Growth-weighted prediction of $\Delta^{18}O_e$ over the course of the experiment
$\Delta^{18}O_{ei}$	Predicted average daytime $\Delta^{18}O_e$ for week i
$\Delta^{18}O_L$	The ^{18}O enrichment of average lamina leaf water compared to source water
$\Delta^{18}O_p$	The ^{18}O enrichment of stem dry matter compared to source water
$\Delta^{18}O_v$	The ^{18}O enrichment of atmospheric water vapor compared to source water
$\delta^{13}C$	The $^{13}C/^{12}C$ ratio relative to the PeeDee Belmnite international standard
$\delta^{13}C_a$	The $\delta^{13}C$ of CO_2 in ambient air
$\delta^{13}C_p$	The $\delta^{13}C$ of plant C
$\delta^{18}O$	The $^{18}O/^{16}O$ ratio relative to Vienna Standard Mean Ocean Water
$\delta^{18}O_p$	The $\delta^{18}O$ of stem dry matter
$\delta^{18}O_s$	The $\delta^{18}O$ of irrigation (source) water

(*Table continues on following page.*)

Table I. (*Continued from previous page.*)

ε_{cp}	The $\delta^{18}O$ difference between plant dry matter and cellulose extracted from it
ε_k	Kinetic $H_2{}^{18}O$ fractionation for diffusion through stomata and leaf boundary layer
ε_{wc}	The ^{18}O enrichment of cellulose compared to the water in which it formed
ε^+	Equilibrium $H_2{}^{18}O$ fractionation during the phase change from liquid to gas
ϕ_c	Proportion of net photosynthesis subsequently used for respiration
ϕ_v	Scaling factor to convert D to v (= v/D)
ϕ_w	Unproductive water loss as proportion of that associated with photosynthesis
$\wp$	Péclet number
ρ	Plant C mass per unit leaf area (mol C m^{-2})

liquid phase diffusion, photorespiration, and dark respiration (Farquhar et al., 1989a). The term d may be excluded from Equation 5, in which case the reduction in $\Delta^{13}C$ caused by d is often accounted for by taking a lower value for b. The $\Delta^{13}C$ is defined with respect to CO_2 in air as $\Delta^{13}C = R_a/R_p - 1$, where R_a is $^{13}C/^{12}C$ of CO_2 in air and R_p is $^{13}C/^{12}C$ of plant C. Combining Equations 5 and 6 gives

$$D \cdot TE_c = \frac{c_a(1-\phi_c)(b-d-\Delta^{13}C)}{1.6\phi_v(1+\phi_w)(b-a)} \quad (7)$$

Equation 7 suggests a negative linear dependence of TE_c (or $D{\cdot}TE_c$) on $\Delta^{13}C$, although it can be seen that there are many other terms in Equation 7 that have the potential to influence the relationship between the two.

O Isotope Enrichment

It has been suggested that measurements of the O isotope enrichment of plant organic material ($\Delta^{18}O_p$) can provide complementary information to that inferred from $\Delta^{13}C$ in analyses of plant water-use efficiency (Farquhar et al., 1989b, 1994; Sternberg et al., 1989; Yakir and Israeli, 1995). Specifically, $\Delta^{18}O_p$ could provide information about the ratio of ambient to intercellular vapor pressures, e_a/e_i, and thus about the leaf-to-air vapor pressure difference, e_i-e_a, during photosynthesis. Note that e_i-e_a is equal to v in Equation 3. In the steady state, water at the evaporative sites in leaves becomes enriched in ^{18}O relative to water entering the plant from the soil, according to the following relationship (Craig and Gordon, 1965; Dongmann et al., 1974; Farquhar and Lloyd, 1993):

$$\Delta^{18}O_e = \varepsilon^+ + \varepsilon_k + (\Delta^{18}O_v - \varepsilon_k)\frac{e_a}{e_i} \quad (8)$$

where $\Delta^{18}O_e$ is the ^{18}O enrichment of evaporative site water relative to source water, ε^+ is the equilibrium fractionation between liquid water and vapor, ε_k is the kinetic fractionation that occurs during diffusion of water vapor out of the leaf, and $\Delta^{18}O_v$ is the discrimination of ambient vapor with respect to source water. The $\Delta^{18}O$ of any water or dry matter component is defined with respect to source water (water entering the roots from the soil) as $\Delta^{18}O = R/R_s - 1$, where $\Delta^{18}O$ is the ^{18}O enrichment of the component of interest and R and R_s are the $^{18}O/^{16}O$ ratios of the component of interest and source water, respectively. The ε^+ can be calculated as a function of leaf temperature (Bottinga and Craig, 1969), and ε_k can be calculated by partitioning the resistance to water vapor diffusion between stomata and boundary layer, with the two weighted by appropriate fractionation factors (Farquhar et al., 1989b; Cappa et al., 2003). The $\Delta^{18}O_v$ can be calculated from measurements of the $\delta^{18}O$ of ambient vapor and source water. If such data are not available, a reasonable approximation is to estimate $\Delta^{18}O_v$ as $-\varepsilon^+$, which means that ambient vapor is assumed to be in isotopic equilibrium with soil water. An up-to-date summary of equations necessary for parameterization of Equation 8 can be found in Cernusak et al. (2007b).

Average lamina leaf water ^{18}O enrichment ($\Delta^{18}O_L$) is generally less than that predicted for evaporative site water (Yakir et al., 1989; Flanagan, 1993; Farquhar et al., 2007), and carbohydrates exported from leaves have been observed to carry the signal of $\Delta^{18}O_L$ rather than $\Delta^{18}O_e$ (Barbour et al., 2000b; Cernusak et al., 2003, 2005; Gessler et al., 2007). The $\Delta^{18}O_L$ has been suggested to relate to $\Delta^{18}O_e$ according to the following relationship (Farquhar and Lloyd, 1993; Farquhar and Gan, 2003):

$$\Delta^{18}O_L = \Delta^{18}O_e\frac{(1-e^{-\wp})}{\wp} \quad (9)$$

where $\wp$ is a Péclet number, defined as $EL/(CD_{18})$, where E is transpiration rate (mol m^{-2} s^{-1}), L is a scaled effective path length (m), C is the molar concentration of water (mol m^{-3}), and D_{18} is the diffusivity of $H_2{}^{18}O$ in water (m^2 s^{-1}). The C is a constant, and D_{18} can be calculated from leaf temperature (Cuntz et al., 2007). The constancy of L, or otherwise, is currently under investigation (Barbour and Farquhar, 2004; Barbour, 2007; Kahmen et al., 2008; Ripullone et al., 2008). If L is assumed relatively constant, Equation 9 predicts that $\Delta^{18}O_L$ will vary as a function of both $\Delta^{18}O_e$ and E. To test for an influence of E on $\Delta^{18}O_L$, it is necessary to first account for variation in $\Delta^{18}O_L$ caused by $\Delta^{18}O_e$ (Flanagan et al., 1994). To this end, the relative deviation of $\Delta^{18}O_L$ from $\Delta^{18}O_e$ ($1 - \Delta^{18}O_L/\Delta^{18}O_e$) can be examined, in which case Equation 9 can be written as

$$1 - \frac{\Delta^{18}O_L}{\Delta^{18}O_e} = 1 - \frac{(1-e^{-\wp})}{\wp} \quad (10)$$

Equation 10 predicts that $1 - \Delta^{18}O_L/\Delta^{18}O_e$ should increase as E increases.

The transfer of the leaf water ^{18}O signal to plant organic material can be described by the following equation (Barbour and Farquhar, 2000):

$$\Delta^{18}O_p = \Delta^{18}O_L(1 - p_{ex}p_x) + \varepsilon_{wc} + \varepsilon_{cp} \quad (11)$$

where $\Delta^{18}O_p$ is ^{18}O enrichment of plant dry matter, p_{ex} is the proportion of O atoms that exchange with local water during synthesis of cellulose, a primary constituent of plant dry matter, p_x is the proportion of unenriched water at the site of tissue synthesis, ε_{wc} is the fractionation between organic oxygen and medium water, and ε_{cp} is the difference in $\Delta^{18}O$ between tissue dry matter and the cellulose component. For tree stems, $p_{ex}p_x$ has been found to be relatively constant at about 0.4 (Roden et al., 2000; Cernusak et al., 2005). The ε_{wc} is relatively constant at about 27‰ (Barbour, 2007), and for stem dry matter, ε_{cp} appears to be relatively constant at about −5‰ (Borella et al., 1999; Barbour et al., 2001; Cernusak et al., 2005). If these assumptions are valid, variation in $\Delta^{18}O_p$ should primarily reflect variation in $\Delta^{18}O_L$. Thus, combining Equations 10 and 11 provides a means of testing for an influence of E on $\Delta^{18}O_p$, assuming that $\Delta^{18}O_p$ provides a time-integrated record of $\Delta^{18}O_L$ (Barbour et al., 2004):

$$1 - \frac{\left(\frac{\Delta^{18}O_p - \varepsilon_{wc} - \varepsilon_{cp}}{1 - p_{ex}p_x}\right)}{\Delta^{18}O_e} = 1 - \frac{(1 - e^{-\wp})}{\wp} \quad (12)$$

RESULTS

Growth, Photosynthesis, and Elemental Concentrations

Daytime meteorological conditions over the course of the experiment are shown in Table II. Dates of initiation of transpiration measurements and harvest for each species are shown in Table III. Table III also shows the initial and final dry masses, in addition to root/shoot ratios. Variation in relative growth rate, r, among species is shown in Figure 1A; variation in the components of r, A, and $1/\rho$, is shown in Figure 1, B and C, respectively. The r varied significantly among functional groups ($P < 0.0001$), and among species within functional groups ($P < 0.0001$). Gymnosperm trees had the lowest mean value of r, whereas angiosperm lianas had the highest mean value; angiosperm trees had a mean value of r intermediate between that of gymnosperm trees and angiosperm lianas (Fig. 1A). In contrast, there was less variation among species and functional groups in instantaneous photosynthesis rates expressed on a leaf area basis (Fig. 1B), although the species *Pinus caribaea* and *Stigmaphyllon hypargyreum* were notable for having relatively high values of A. Variation in r tended to be more closely associated with variation in $1/\rho$ than with variation in A. Gymnosperm trees had the lowest mean value of $1/\rho$, whereas angiosperm trees had an intermediate mean value, and angiosperm lianas had the highest mean value (Fig. 1C). The liana species *S. hypargyreum* possessed swollen, tuberous roots, which caused it to have a root/shoot ratio much higher than any other species in the study (Table III), and to have a reduced $1/\rho$ relative to the other two liana species (Fig. 1C).

Variation in instantaneous photosynthesis, when expressed on a leaf mass basis, was a good predictor of variation in r (Fig. 2). The former was measured over several minutes, whereas the latter was measured over several months. Mass-based photosynthesis, A_m, is the product of A (mol m^{-2} s^{-1}) and specific leaf area (SLA; m^2 kg^{-1}). The correlation between A_m and r was almost entirely driven by variation in SLA, because A on a leaf area basis was not significantly correlated with r ($P = 0.14$, $n = 94$).

The C and N concentrations of leaves, stems, roots, and whole plants for each species are given in Supplemental Table S1. For whole-plant C concentration, there was significant variation, both among functional groups ($P < 0.0001$), and among species within functional groups ($P < 0.0001$), as shown in Figure 3A. Gymnosperm trees had a mean C concentration of 49.6%, significantly higher than angiosperm trees and lianas. Angiosperm trees and lianas did not differ from each other in whole-plant C concentration, and had mean values of 45.4% and 44.9%, respectively. For whole plant N concentration, there was also significant variation among functional groups ($P < 0.0001$) and among species within functional groups ($P < 0.0001$), as shown in Figure 3B. Angiosperm lianas had the highest mean whole-plant N concentration at 1.22%, followed by angiosperm trees at 1.01%, then by gymnosperm trees at 0.82%. Accordingly, there was significant variation among functional groups ($P < 0.0001$) and

Table II. *Average daytime meteorological conditions at the study site over the course of the experiment*

Values are monthly means of measurements taken every 15 min between the hours of 7 AM and 5:30 PM local time. We focused on daytime hours to characterize conditions during photosynthetic gas exchange.

	2005							2006				
	June	July	Aug	Sept	Oct	Nov	Dec	Jan	Feb	March	April	May
Air temperature (°C)	28.0	26.7	28.6	29.6	30.0	27.7	30.7	28.1	27.9	29.1	28.7	28.2
Relative humidity (%)	81.3	82.9	82.6	83.3	79.3	84.2	75.0	72.5	68.8	68.3	74.1	80.1
Vapor pressure deficit (kPa)	0.73	0.62	0.71	0.70	0.89	0.60	1.12	1.06	1.18	1.31	1.03	0.78
Wind speed (m s^{-1})	0.33	0.26	0.31	0.33	0.45	0.29	0.50	0.61	0.87	0.82	0.75	0.38
Photon flux density (μmol m^{-2} s^{-1})	685	655	649	628	750	602	743	808	859	925	854	685

Table III. *Experimental time period, initial and final plant dry mass, and root to shoot ratio for each species in the study*

Values for final dry mass and root to shoot ratio are given as the mean, with the SD in parentheses. An SD is not given for *P. guatemalensis* because only one plant survived for this species. Full species names are given in Figure 2. NA, Not applicable.

Species	Family	Start Date	End Date	No. of Plants	Initial Dry Mass	Final Dry Mass	Root to Shoot Ratio
					g	*g*	*g g*$^{-1}$
Gymnosperm tree species							
C. lusitanica	Cupressaceae	May 23, 2005	Dec. 13, 2005	8	5.8	60.2 (19.0)	0.36 (0.06)
P. caribaea	Pinaceae	May 23, 2005	Dec. 13, 2005	8	5.6	64.6 (30.9)	0.27 (0.09)
P. guatemalensis	Podocarpaceae	May 23, 2005	May 11, 2006	1	0.8	107.3 (NA)	0.16 (NA)
T. occidentalis	Cupressaceae	April 26, 2004	Dec. 13, 2005	8	4.7	41.4 (16.5)	0.47 (0.08)
Angiosperm tree species							
C. longifolium	Clusiaceae	July 11, 2005	March 10, 2006	6	3.1	62.6 (27.0)	0.39 (0.08)
C. pratensis	Clusiaceae	Aug. 22, 2005	May 11, 2006	6	0.2	112.2 (62.3)	0.76 (0.26)
H. alchorneoides	Euphorbiaceae	June 20, 2005	Dec. 13, 2005	6	0.2	36.6 (30.2)	1.10 (0.13)
L. seemannii	Tiliaceae	Aug. 29, 2005	March 10, 2006	7	0.1	39.8 (7.3)	0.61 (0.10)
P. pinnatum	Fabaceae	Nov. 7, 2005	March 10, 2006	2	0.6	53.9 (16.6)	0.58 (0.20)
P. pinnatum	Fabaceae	Nov. 7, 2005	May 11, 2006	3	0.6	21.6 (13.3)	0.36 (0.14)
S. macrophylla	Meliaceae	Nov. 7, 2005	May 11, 2006	7	0.8	24.3 (11.8)	0.34 (0.10)
T. rosea	Bignoniaceae	June 20, 2005	Dec. 13, 2005	6	0.6	64.8 (11.0)	0.92 (0.12)
T. grandis	Verbenaceae	May 17, 2004	May 11, 2006	7	0.1	45.5 (11.3)	0.93 (0.17)
Angiosperm liana species							
G. lupuloides	Rhamnaceae	Aug. 29, 2005	March 10, 2006	6	0.01	31.5 (15.6)	0.47 (0.20)
M. leiostachya	Asteraceae	Aug. 29, 2005	March 10, 2006	3	0.1	21.2 (4.3)	0.37 (0.27)
M. leiostachya	Asteraceae	Nov. 14, 2005	May 11, 2006	3	0.3	23.2 (4.8)	0.25 (0.06)
S. hypargyreum	Malphigiaceae	Aug. 29, 2005	March 10, 2006	7	0.1	50.3 (20.3)	1.99 (0.21)

among species within functional groups ($P < 0.0001$) in whole-plant C/N mass ratio (Fig. 3C). Gymnosperm trees had the highest mean whole-plant C/N at 64.7 g g^{-1}, followed by angiosperm trees at 49.6 g g^{-1}, then by angiosperm lianas at 39.0 g g^{-1}.

Concentrations of phosphorus (P), calcium (Ca), and potassium (K), and the N/P mass ratio in leaf dry matter for each species are shown in Table IV. There was significant variation among functional groups ($P < 0.0001$) and among species within functional groups ($P < 0.0001$) for all elements and for N/P. Angiosperm lianas tended to have higher mean concentrations of P, Ca, and K in their leaf dry matter than angiosperm and gymnosperm trees. The mean leaf N/P was higher in angiosperm trees than in gymnosperm trees or angiosperm lianas; mean values were 9.3, 4.9, and 4.7 g g^{-1}, respectively.

When expressed on a leaf area basis, the leaf P concentration was significantly correlated with mean transpiration rate (MTR) across all individuals ($R^2 = 0.24$, $P < 0.0001$, $n = 94$). The equation relating the two was $P_{area} = 0.096\text{MTR} + 2.75$, where P_{area} is in mmol m^{-2}, and MTR is in mol m^{-2} d^{-1}.

NUE

Equation 2 presents a means for analyzing variation among functional groups and species in whole-plant NUE (mol C mol^{-1} N s^{-1}). We calculated NUE as the product of r and m_c/m_n, the whole-plant C to N molar ratio; thus, a relatively high C/N has the effect of increasing NUE. Figure 4A shows variation among species in NUE. There was significant variation among

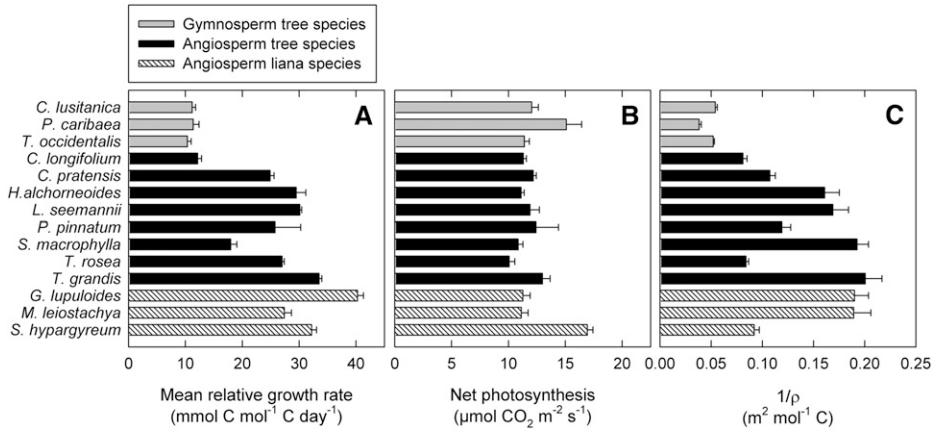

Figure 1. A to C, Variation among species in mean relative growth rate (A), net photosynthesis, expressed on a leaf area basis (B), and leaf area per unit plant C mass, 1/ρ (C). Error bars represent 1 SE. Sample sizes for each species are given in Table III.

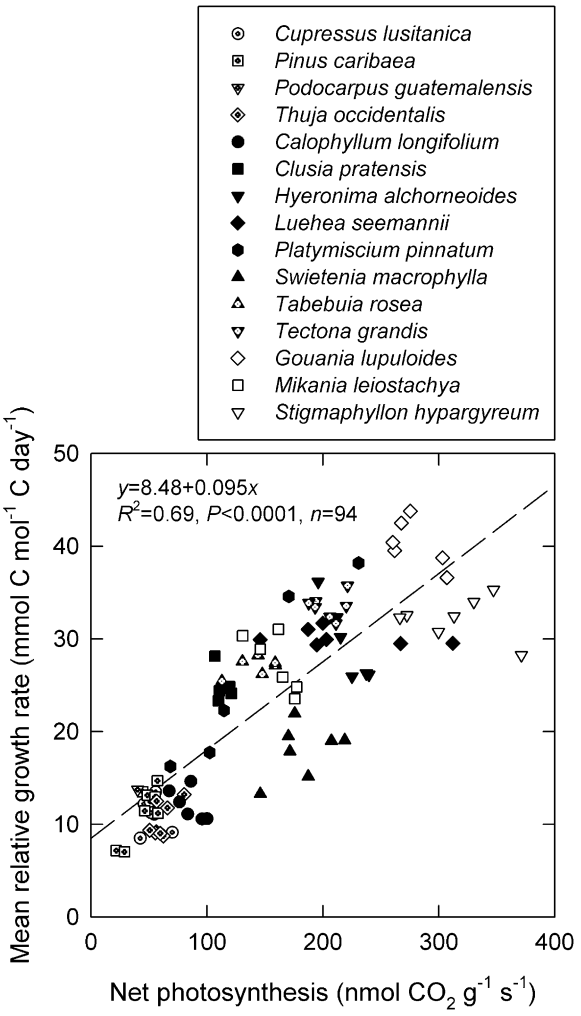

Figure 2. Mean relative growth rate plotted against instantaneous measurements of photosynthesis expressed on a leaf mass basis. White symbols with internal cross-hairs refer to gymnosperm tree species; completely white symbols refer to angiosperm liana species; black symbols and black symbols with internal cross-hairs refer to angiosperm tree species.

functional groups ($P < 0.0001$) and among species within functional groups ($P < 0.0001$). However, unlike results for r, angiosperm trees and lianas did not differ from each other with respect to NUE ($P = 0.84$). In contrast, NUE of gymnosperm trees was lower than that of both angiosperm trees ($P < 0.0001$) and angiosperm lianas ($P < 0.0001$). Figure 4, B and C, shows variation among species in the NUE components, A_n and n_l. Variation in NUE among species tended to reflect variation in A_n, the photosynthetic NUE (Fig. 4B). The A_n was also higher in angiosperm trees and lianas than in gymnosperm trees (Fig. 4B). This variation in A_n was offset to a lesser extent by variation in n_l, the proportion of plant N allocated to leaves (Fig. 4C). Gymnosperm trees had highest mean n_l, at 0.69, followed by angiosperm trees at 0.59, then by angiosperm lianas at 0.50. Thus, a higher allocation of N to leaves in gymnosperm trees compensated to some extent for their much lower A_n. However, the A_n was still the dominant control over NUE (Fig. 5).

Transpiration Efficiency

Mean values for each species for TE_c, the whole-plant transpiration efficiency of C gain, are shown in Table V. Also shown in Table V are the growth-weighted estimates of the daytime vapor pressure deficit, D_g, by species. There was significant variation, both among functional groups ($P < 0.0001$), and among species within functional groups ($P < 0.0001$), in both TE_c and D_g. However, across the full data set, TE_c and D_g were not significantly correlated ($P = 0.11$, $n = 94$), suggesting that D_g was not a primary control over TE_c. Taking the product of D_g and TE_c allows analysis of variation in TE_c independently of variation in D_g, as articulated in Equation 5. The $D_g \cdot TE_c$ also varied significantly among functional groups ($P < 0.0001$) and among species within functional groups ($P < 0.0001$). Angiosperm trees had the highest mean $D_g \cdot TE_c$ at 1.58 Pa mol C mol^{-1} H_2O, followed by angiosperm lianas at 1.30 Pa mol C mol^{-1} H_2O, then by gymnosperm trees at 1.11 Pa mol C mol^{-1} H_2O. Among all species, there was a 3.7-fold variation in $D_g \cdot TE_c$ (i.e. the largest species mean was 3.7 times the smallest species mean).

Table V summarizes for each species the components of $D_g \cdot TE_c$ that we quantified: ϕ_v, the ratio of leaf-to-air vapor pressure difference to air vapor pressure deficit; ϕ_w, the ratio of unproductive to productive water loss; and c_i/c_a, the ratio of intercellular to ambient CO_2 partial pressures during photosynthesis. Although there was a 1.8-fold variation among species in ϕ_v, this parameter did not appear to be a primary control over $D_g \cdot TE_c$: the term $1/\phi_v$ explained only 13% of variation in $D_g \cdot TE_c$ ($R^2 = 0.13$, $P = 0.0004$, $n = 94$); moreover, the slope of the relationship between $D_g \cdot TE_c$ and $1/\phi_v$ was negative, opposite to that predicted by Equation 5. The parameter ϕ_w similarly did not appear to exert a strong control over $D_g \cdot TE_c$: although $D_g \cdot TE_c$ was positively correlated with $1/(1 + \phi_w)$ ($R^2 = 0.18$, $P < 0.0001$, $n = 92$), there was only a 1.1-fold variation in this term among species, suggesting that it could only account for a variation in $D_g \cdot TE_c$ of approximately 10%. In contrast, the c_i/c_a appeared to be the primary control over $D_g \cdot TE_c$. Among species, there was a 2.3-fold variation in instantaneous measurements of $1 - c_i/c_a$, and c_i/c_a explained 46% of variation in $D_g \cdot TE_c$. Regression coefficients are given in Table VI. Furthermore, instantaneous measurements of $1 - c_i/c_a$ explained 64% of variation in the composite term $v_g \cdot TE_c(1 + \phi_w)$ ($R^2 = 0.64$, $P < 0.0001$, $n = 94$). Taking this product means that only the variables ϕ_c, c_a, and c_i/c_a remain on the right side of Equation 5.

Variation in instantaneous measurements of c_i/c_a was largely driven by variation in stomatal conductance, g_s, rather than by variation in photosynthesis, A. If g_s

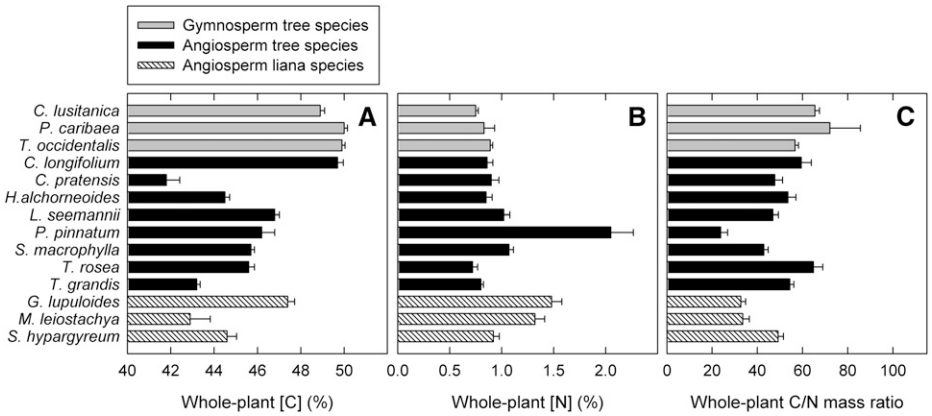

Figure 3. A to C, Variation among species in the C concentration of dry matter on a whole-plant basis (A), the N concentration of dry matter on a whole-plant basis (B), and the C/N mass ratio of dry matter on a whole-plant basis (C). Error bars represent 1 SE. Sample sizes for each species are given in Table III.

controls variation in c_i/c_a, then c_i/c_a should decrease as $1/g_s$ increases. The $1/g_s$ is equivalent to the stomatal resistance. In contrast, if A controls c_i/c_a, then c_i/c_a should decrease as A increases. Figure 6A shows that instantaneous c_i/c_a decreased as a linear function of $1/g_s$. In contrast, Figure 6B shows that there was a weak tendency for c_i/c_a to increase as A increased, opposite to the trend that would be expected if A were controlling c_i/c_a.

We used measurements of leaf temperature, taken with a hand-held infrared thermometer, to calculate values of ϕ_v for the species harvested on the second and third harvest dates (Table III). We then compared these instantaneous measurements of ϕ_v with our time-integrated estimates for each plant based on leaf energy balance predictions and meteorological data. The time-integrated estimates of ϕ_v compared favorably with the instantaneous measurements of ϕ_v ($R^2 = 0.42$, $P < 0.0001$, $n = 55$), thus providing some validation of the former.

Stable Isotope Composition

The C isotope composition of leaves, stems, roots, and whole plants is shown for each species in Table VII. Also shown is the difference in $\delta^{13}C$ between leaves and the sum of stems plus roots, the heterotrophic component of the plant. Across all individuals, leaf $\delta^{13}C$ was more negative than stem $\delta^{13}C$ ($P < 0.0001$, $n = 94$) and root $\delta^{13}C$ ($P < 0.0001$, $n = 94$), whereas stem $\delta^{13}C$ was more negative than root $\delta^{13}C$, but by a much smaller amount ($P = 0.0008$, $n = 94$); mean values for leaf, stem, and root $\delta^{13}C$ were -29.4, -28.1, and $-27.8‰$, respectively.

Table IV. *Leaf P, Ca, and K concentrations, and N/P ratios of experimental plants*

Values are given as the mean for each species, with the SD in parentheses. No SD is given for *P. guatemalensis* because only one individual of this species survived. Sample sizes for the other species ranged from five to eight individuals, as shown in Table III. NA, Not applicable.

Species	P	Ca	K	N/P
	$g\ kg^{-1}$	$g\ kg^{-1}$	$g\ kg^{-1}$	$g\ g^{-1}$
Gymnosperm tree species				
C. lusitanica	3.10 (0.76)	8.3 (0.9)	20.9 (2.8)	3.6 (0.8)
P. caribaea	1.43 (0.47)	3.6 (1.4)	9.6 (1.6)	7.6 (1.4)
P. guatemalensis	2.48 (NA)	8.1 (NA)	16.9 (NA)	5.9 (NA)
T. occidentalis	4.24 (0.86)	10.5 (2.2)	16.8 (1.5)	3.4 (0.8)
Angiosperm tree species				
C. longifolium	0.94 (0.23)	7.7 (0.8)	8.4 (1.4)	12.4 (1.5)
C. pratensis	1.38 (0.47)	13.6 (1.1)	14.4 (5.2)	9.7 (2.1)
H. alchorneoides	2.22 (0.59)	12.5 (3.9)	24.0 (4.3)	6.8 (1.5)
L. seemannii	3.59 (0.81)	18.0 (2.1)	14.2 (1.6)	5.0 (1.4)
P. pinnatum	1.68 (0.23)	10.2 (2.1)	16.7 (4.3)	18.2 (5.7)
S. macrophylla	1.33 (0.35)	13.4 (1.5)	20.3 (3.0)	12.0 (2.8)
T. rosea	1.43 (0.04)	14.4 (4.3)	15.1 (4.4)	11.1 (2.2)
T. grandis	5.96 (0.42)	8.6 (1.0)	13.3 (2.1)	2.0 (0.2)
Angiosperm liana species				
G. lupuloides	5.33 (1.15)	14.4 (2.1)	24.5 (2.4)	4.4 (0.9)
M. leiostachya	2.66 (0.30)	13.2 (1.4)	29.5 (3.5)	6.6 (1.2)
S. hypargyreum	6.23 (1.09)	23.4 (3.3)	24.6 (4.0)	3.5 (0.5)

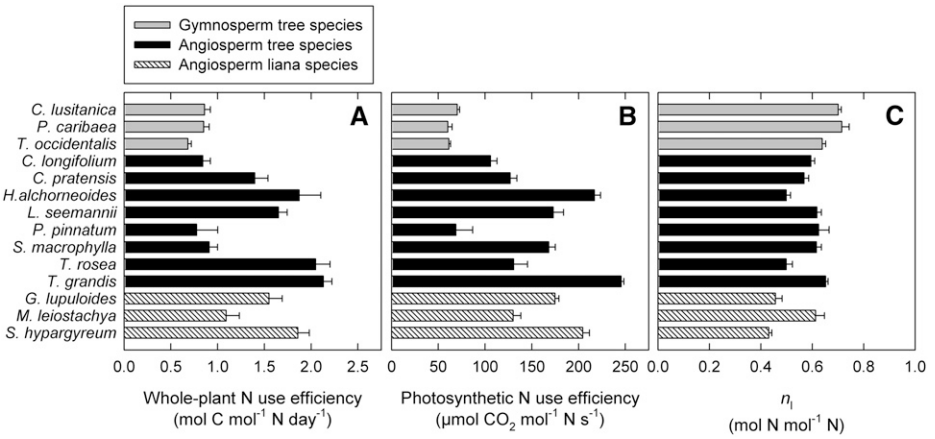

Figure 4. A to C, Variation among species in whole-plant NUE (A), photosynthetic NUE (B), and n_l, the leaf N content as a proportion of whole-plant N content (C). Error bars represent 1 SE. Sample sizes for each species are given in Table III.

We converted plant $\delta^{13}C$ values to ^{13}C discrimination by assuming $\delta^{13}C$ of atmospheric CO_2 to be $-8‰$. Whole-plant $\Delta^{13}C$, $\Delta^{13}C_p$, covered a range from 18.8‰ to 22.9‰ among species, corresponding to $\delta^{13}C_p$ values ranging from $-26.3‰$ to $-30.2‰$ (Table VII). There was significant variation in $\Delta^{13}C_p$ among functional groups ($P = 0.002$) and among species within functional groups ($P < 0.0001$). The $\Delta^{13}C_p$ was lower in angiosperm trees than in gymnosperm trees, whereas angiosperm lianas did not differ significantly from angiosperm or gymnosperm trees. Mean values were 21.0‰, 21.2‰, and 21.5‰ for angiosperm trees, angiosperm lianas, and gymnosperm trees, respectively.

The $\Delta^{13}C_p$ was significantly correlated with instantaneous measurements of c_i/c_a (Fig. 7), as predicted by Equation 6. We estimated the term d of Equation 6 by least-squares regression by assuming fixed values for a and b of 4.4‰ and 29‰, respectively. This resulted in an estimate for d of 3.1‰; the regression equation explained 57% of variation in $\Delta^{13}C_p$. Thus, the predictive power of this relationship was equivalent to that obtained with a standard linear regression, in which both the slope and intercept are free to vary (Fig. 7). Using the mean estimate of 3.1‰ for d, and values of 4.4‰ and 29‰ for a and b, respectively, we calculated a $\Delta^{13}C_p$-based estimate of c_i/c_a for each plant. Mean values of these estimates for each species are given in Table V. There was a 2.4-fold variation among species in the $\Delta^{13}C_p$-based estimates of $1 - c_i/c_a$.

Variation in $\Delta^{13}C_p$ was significantly correlated with variation in $D_g \cdot TE_c$ (Fig. 8); the former explained 49% of variation in the latter. Regression coefficients and the coefficient of determination for least-squares linear regressions of TE_c, $D_g \cdot TE_c$, and $v_g \cdot TE_c$ against $\Delta^{13}C$ of leaves, stems, roots, and whole plants are given in Table VI. In general, whole-plant $\Delta^{13}C$ was a better predictor of variation in TE_c than $\Delta^{13}C$ of leaves, stems, or roots individually. Additionally, weighting of TE_c by D_g or v_g tended to result in modest increases in the proportion of variation explained by the regression models (Table VI).

Correlations between $\Delta^{13}C_p$ and $1/g_s$ and A further supported the conclusion that variation in c_i/c_a was largely driven by variation in g_s. The $\Delta^{13}C_p$ decreased as a linear function of $1/g_s$ (Fig. 6C). In contrast, the $\Delta^{13}C_p$ showed a weak tendency to increase as a function of A (Fig. 6D), opposite to the trend that would be expected if A controlled variation in c_i/c_a.

Variation among species in the O isotope composition of stem dry matter is given in Table VII. We calculated the ^{18}O enrichment above source water of stem dry matter, $\Delta^{18}O_p$, from the mean $\delta^{18}O$ of irrigation water of $-4.3‰$. The observed $\Delta^{18}O_p$ was significantly correlated with the predicted ^{18}O enrichment of evaporative site water, $\Delta^{18}O_e$, weighted by predicted weekly growth increments (Fig. 9). We tested whether the residual variation in $\Delta^{18}O_p$, after accounting for variation in $\Delta^{18}O_e$, was related to transpiration rate by plotting $1 - [(\Delta^{18}O_p - \varepsilon_{wc} - \varepsilon_{cp})/(1 - p_{ex}p_x)]/\Delta^{18}O_e$ against the MTR. As shown in Equation 12, this term should increase with an increasing transpiration rate if there is a significant Péclet effect. Our analysis detected a significant relationship between the two

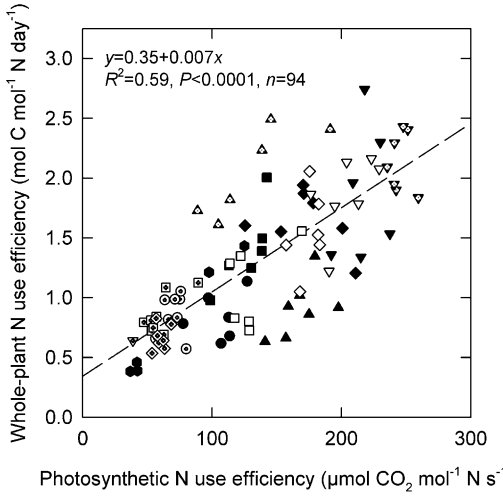

Figure 5. Whole-plant NUE plotted against photosynthetic NUE. Whole-plant NUE was calculated from mean relative growth rate, measured over several months, whereas photosynthetic NUE was calculated from instantaneous photosynthesis measurements, taken over several minutes. Different symbols refer to different species, as detailed in Figure 2.

Table V. *Transpiration efficiency and related parameters for each species*

Symbol definitions are as follows: transpiration efficiency of C uptake (TE_c); growth-weighted daytime vapor pressure deficit (D_g) and leaf-to-air vapor pressure difference (v_g); the ratio of nighttime to daytime transpiration (E_n/E_d); and the ratio of intercellular to ambient CO_2 partial pressures (c_i/c_a). The c_i/c_a is given as the value measured with a portable photosynthesis system (instantaneous), or as the value estimated from whole-plant ^{13}C discrimination ($\Delta^{13}C_p$-based). Values are given as the mean for each species, with the SD in parentheses. No SD is given for *P. guatemalensis* because only one individual of this species survived. Sample sizes for the other species ranged from five to eight individuals, as shown in Table III. NA, Not applicable.

Species	TE_c	D_g	v_g	ϕ_v (= v_g/D_g)	ϕ_w (= E_n/E_d)	Instantaneous c_i/c_a	$\Delta^{13}C_p$-Based c_i/c_a
	mmol C mol^{-1} H_2O	*kPa*	*kPa*				
Gymnosperm tree species							
C. lusitanica	1.29 (0.20)	0.76 (0.01)	0.90 (0.07)	1.17 (0.08)	0.11 (0.02)	0.78 (0.04)	0.80 (0.02)
P. caribaea	1.20 (0.19)	0.76 (0.01)	0.72 (0.05)	0.95 (0.07)	0.04 (0.02)	0.86 (0.03)	0.88 (0.02)
P. guatemalensis	3.48 (NA)	1.04 (NA)	1.71 (NA)	1.64 (NA)	0.04 (NA)	0.63 (NA)	0.63 (NA)
T. occidentalis	1.85 (0.19)	0.76 (0.01)	0.92 (0.03)	1.21 (0.05)	0.03 (0.03)	0.80 (0.02)	0.78 (0.01)
Angiosperm tree species							
C. longifolium	1.83 (0.24)	1.05 (0.02)	1.53 (0.12)	1.46 (0.10)	0.04 (0.04)	0.76 (0.04)	0.78 (0.05)
C. pratensis	2.16 (0.22)	1.02 (0.01)	1.42 (0.06)	1.39 (0.06)	0.01 (0.01)	0.76 (0.03)	0.73 (0.01)
H. alchorneoides	1.50 (0.20)	0.83 (0.01)	1.37 (0.04)	1.65 (0.05)	0.08 (0.01)	0.80 (0.02)	0.85 (0.01)
L. seemannii	0.98 (0.15)	1.20 (0.00)	1.43 (0.20)	1.19 (0.16)	0.05 (0.01)	0.80 (0.03)	0.81 (0.02)
P. pinnatum	2.76 (0.62)	1.12 (0.10)	1.53 (0.28)	1.39 (0.36)	0.02 (0.01)	0.73 (0.09)	0.71 (0.06)
S. macrophylla	1.07 (0.22)	1.05 (0.01)	1.21 (0.03)	1.15 (0.03)	0.07 (0.01)	0.86 (0.02)	0.88 (0.02)
T. rosea	1.92 (0.24)	0.82 (0.00)	1.37 (0.18)	1.67 (0.21)	0.11 (0.02)	0.75 (0.06)	0.79 (0.03)
T. grandis	0.84 (0.07)	0.98 (0.01)	1.20 (0.08)	1.23 (0.09)	0.08 (0.01)	0.88 (0.03)	0.81 (0.03)
Angiosperm liana species							
G. lupuloides	0.96 (0.34)	1.25 (0.01)	1.37 (0.08)	1.10 (0.06)	0.04 (0.01)	0.84 (0.03)	0.80 (0.02)
M. leiostachya	0.89 (0.23)	1.11 (0.10)	1.39 (0.20)	1.25 (0.12)	0.07 (0.02)	0.79 (0.05)	0.80 (0.06)
S. hypargyreum	1.35 (0.14)	1.21 (0.01)	1.18 (0.06)	0.97 (0.05)	0.03 (0.01)	0.82 (0.03)	0.82 (0.02)

parameters ($R^2 = 0.14$, $P = 0.0002$, $n = 94$), supporting the notion of a significant Péclet effect, although there was considerable scatter in the relationship. Using the MTR and E_n/E_d, we calculated a daytime MTR, then used the nonlinear regression routine in SYSTAT to solve for an average value of L, the scaled effective path length, across the full data set. This analysis estimated a mean value of L for the full data set of 53 mm, with the 95% confidence interval ranging from 43 to 62 mm.

DISCUSSION

In this article, we present a comprehensive comparison of physiological processes in seedlings of conifers, angiosperm trees, and angiosperm lianas under tropical field conditions. The comparison yielded novel insights into physiological differences among these functional groups, when grown in a tropical environment. For example, we observed that liana species, on average, had higher $1/\rho$ than tree species, and that this trait was associated with faster growth. We also observed that gymnosperm trees had significantly lower whole-plant NUE than both angiosperm trees and angiosperm lianas. In addition, the results provided an integrated account of the physiological controls over growth, whole-plant water and NUE, and stable isotope composition across the full range of species. Relative growth rate, r, was mainly controlled by variation in $1/\rho$, the amount of assimilative surface area for a given plant biomass (Fig. 1). Of the components of $1/\rho$, the SLA played a key role, such that the product of SLA and instantaneous photosynthesis, A, was a strong predictor of variation in r (Fig. 2). The whole-plant NUE was mainly controlled by A_n, the photosynthetic rate for a given amount of leaf N (Fig. 5). An increase in the proportional allocation of N to leaves, n_l, in species with low A_n was observed; however, the increased n_l compensated to only a relatively modest extent for low A_n (Fig. 4). The primary control over the transpiration efficiency of C uptake, TE_c, was c_i/c_a, the ratio of intercellular to ambient CO_2 partial pressures during photosynthetic gas exchange (Tables V and VI). The c_i/c_a was also the primary control over whole-plant ^{13}C discrimination, $\Delta^{13}C_p$ (Fig. 7), such that variation in $\Delta^{13}C_p$ was closely correlated with variation in TE_c (Table VI; Fig. 8). The c_i/c_a, in turn, was largely controlled by stomatal conductance, g_s (Fig. 6). The ^{18}O enrichment of stem dry matter, $\Delta^{18}O_p$, was primarily controlled by the predicted ^{18}O enrichment of the evaporative sites within leaves, $\Delta^{18}O_e$, during photosynthetic gas exchange (Fig. 9). Variation in leaf transpiration rate further explained some of the residual variation in $\Delta^{18}O_p$ not accounted for by variation in $\Delta^{18}O_e$.

Growth and NUE

We observed that the term $1/\rho$ was the primary control over variation in r, and that A was a relatively conservative parameter among species (Fig. 1). These

Table VI. *The proportion of variation in transpiration efficiency explained by ^{13}C discrimination and instantaneous c_i/c_a*

Linear regression equations were fitted with the following parameters alternatively used as dependent variables: transpiration efficiency of C uptake (TE_c); the product of TE_c and growth-weighted vapor pressure deficit ($D_g \cdot TE_c$); and the product of TE_c and growth-weighted leaf-to-air vapor pressure difference ($v_g \cdot TE_c$). Independent variables were whole-plant ^{13}C discrimination ($\Delta^{13}C$); $\Delta^{13}C$ of leaves, stems, or roots individually; and instantaneous c_i/c_a. For each analysis, $n = 94$. All regression coefficients were significant at $P < 0.0001$.

Dependent Variable	Regression Coefficient						Model R^2
	Intercept	Whole-Plant $\Delta^{13}C$ ‰	Leaf $\Delta^{13}C$ ‰	Stem $\Delta^{13}C$ ‰	Root $\Delta^{13}C$ ‰	Instantaneous c_i/c_a	
TE_c	7.76	−0.298					0.45
$D_g \cdot TE_c$	8.40	−0.330					0.49
$v_g \cdot TE_c$	14.4	−0.594					0.53
TE_c	7.04		−0.253				0.38
$D_g \cdot TE_c$	8.03		−0.300				0.48
$v_g \cdot TE_c$	12.9		−0.501				0.45
TE_c	6.87			−0.262			0.40
$D_g \cdot TE_c$	7.42			−0.290			0.45
$v_g \cdot TE_c$	12.8			−0.528			0.50
TE_c	6.66				−0.255		0.36
$D_g \cdot TE_c$	6.53				−0.251		0.32
$v_g \cdot TE_c$	11.8				−0.487		0.40
TE_c	7.30					−7.27	0.51
$D_g \cdot TE_c$	7.21					−7.20	0.46
$v_g \cdot TE_c$	13.6					−14.6	0.62

results agree with those presented previously for 24 herbaceous species (Poorter and Remkes, 1990; Poorter et al., 1990), and for many woody species (Cornelissen et al., 1996; Atkin et al., 1998; Wright and Westoby, 2000). For the herbaceous species, SLA was also a key component of $1/\rho$, such that variation in r was not correlated with variation in A, but was strongly correlated with variation in A_m, the product of A and SLA (Poorter et al., 1990). It should be noted that A was measured near the end of the experiment, and our results thus do not preclude the possibility that variation in A may have modulated r earlier in plant development. Nonetheless, our measurements of A_m explained more than two-thirds of total variation in r (Fig. 2). Among the species that we grew, the gymnosperm trees generally had lowest $1/\rho$ and r, whereas angiosperm lianas had highest $1/\rho$ and r, with angiosperm trees intermediate between the two (Fig. 1). This pattern suggests that variation in $1/\rho$ could be related to hydraulic efficiency, with the tracheid-bearing gymnosperm species constrained by a lower hydraulic conductance for a given plant mass, and thereby requiring a greater plant mass to support a given amount of assimilative, and thus evaporative, surface area. On the other hand, the angiosperm liana species, having freed themselves from the constraint of structural self-sufficiency, and possessing hydraulically efficient vessels, might then have required a smaller plant mass to deliver water to a given leaf surface area. Measurements of whole-plant hydraulic conductance per unit plant mass would be necessary to confirm this hypothesis. However, it would be consistent with differences in hydraulic conductivity observed previously between gymnosperm and angiosperm seedlings (Brodribb et al., 2005).

As shown in Equation 1, the term ϕ_c, the proportion of net C fixation used for respiration, has potential to influence r. It was previously observed for 24 herbaceous species that ϕ_c ranged from about 0.5 to 0.3, and that r was negatively correlated with ϕ_c, as predicted by Equation 1 (Poorter et al., 1990). Although we did not measure ϕ_c in our study, we can speculate that the slower-growing species had higher values, because they generally had higher whole-plant C concentrations (Fig. 3A), which would correlate with higher tissue construction costs (Vertregt and Penning de Vries, 1987; Poorter, 1994). The r was negatively correlated with whole-plant C concentration across the full data set ($R^2 = 0.35$, $P < 0.0001$, $n = 94$).

The leaf N/P mass ratios that we observed (Table IV) were generally low for tropical vegetation (Reich and Oleksyn, 2004). However, they are consistent with a previous study conducted under similar conditions, but with variable amounts of rice (*Oryza sativa*) husk mixed into the experimental soil (Cernusak et al., 2007b). At a similar rice husk/soil mixture as used in this study, we previously observed a mean leaf N/P ratio of 5.9 for *Ficus insipida* (Cernusak et al., 2007b), whereas the overall mean for all species in this study was 7.2. The generally low leaf N/P ratios suggest that plant growth in this study was constrained primarily by N availability, rather than by P availability (Koerselman and Meuleman, 1996; Aerts and Chapin, 2000). This is consistent with the addition of rice husks increasing the C/N ratio of the experimental soil, thereby favoring microbial immobilization of soil N,

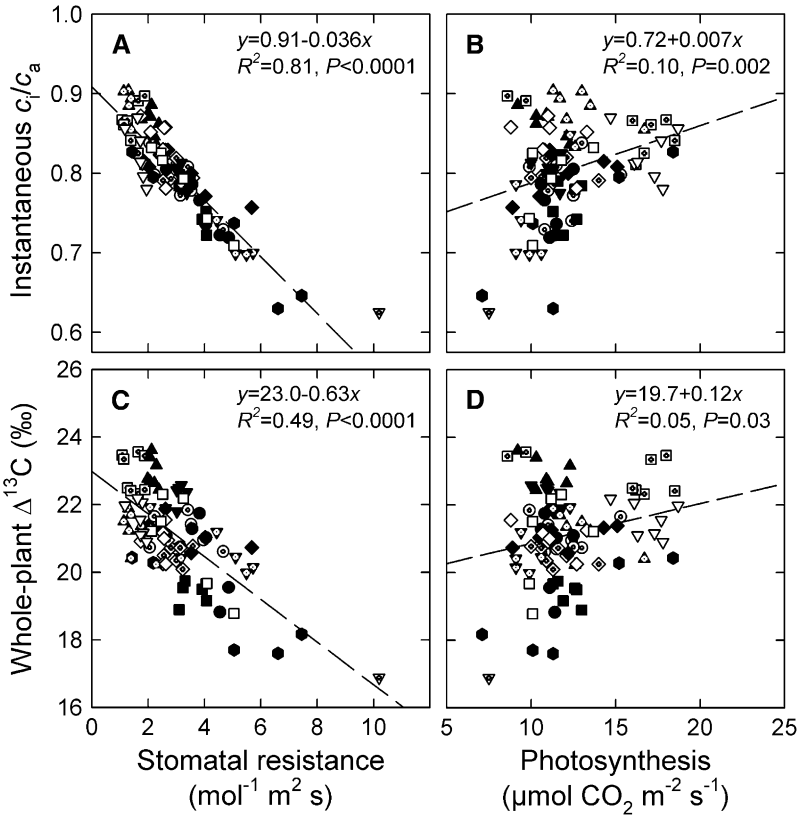

Figure 6. A to D, The top two panels show instantaneous measurements of c_i/c_a plotted against stomatal resistance (A) and photosynthesis (B); the bottom two panels show whole-plant ^{13}C discrimination plotted against stomatal resistance (C) and photosynthesis (D). Stomatal resistance is the inverse of stomatal conductance. Different symbols refer to different species, as described for Figure 2.

and thus reducing N availability to plants. This provided a useful experimental basis for comparing NUE among the species in our study, because N was likely the nutrient most limiting plant growth.

We calculated whole-plant NUE as the product of r and m_c/m_n, the whole-plant molar ratio of C to N. Although the gymnosperm species had higher C/N than the angiosperm species (Fig. 4), they were still at a marked disadvantage with respect to NUE. Such disadvantage resulted primarily from a lower A_n (Figs. 4 and 5). This difference between gymnosperm and angiosperm seedlings, whereby the former employed N much less efficiently than the latter for accumulating C, could be decisive in determining competitive outcomes between the two. Although productivity in tropical forests is generally considered P limited, it has also been reported that N availability can constrain tree growth in both montane (Tanner et al., 1998) and lowland (LeBauer and Treseder, 2008) tropical forests. Thus, a higher NUE may contribute to angiosperm dominance in tropical environments. The low A_n in the gymnosperm species compared to the angiosperm species resulted primarily from lower SLA, because A was generally similar between the two groups, and leaf N concentration was lower in gymnosperms than in angiosperms (Supplemental Table S1).

Transpiration Efficiency

The species included in the study exhibited a large variation in the transpiration efficiency of C uptake, TE_c (Table V). This is consistent with previous results showing large variation in TE_c among seven tropical tree species (Cernusak et al., 2007a). When the TE_c for each individual plant was normalized according to its growth-weighted mean daytime vapor pressure deficit, D_g, the variation among species was still apparent, suggesting that D_g was not a primary control over TE_c. Additionally, the relative ranking among species in this study was consistent with results for three species that were also measured previously (Cernusak et al., 2007a); in this study *Platymiscium pinnatum* had the highest $D_g \cdot TE_c$, *Swietenia macrophylla* an intermediate value, and *Tectona grandis* the lowest value (3.05, 1.12, and 0.82 Pa mol C mol^{-1} H_2O, respectively). Previously, we observed that TE_c for these three species was 3.97, 2.88, and 1.63 mmol C mol^{-1} H_2O, respectively (Cernusak et al., 2007a).

In this study, we were able to confirm that c_i/c_a was the primary control over $D_g \cdot TE_c$. The ϕ_v also showed a moderate variation among species, suggesting that it could be an important source of variation in $D_g \cdot TE_c$ (Table V); however, the ϕ_v tended to be negatively correlated with c_i/c_a, due to a mutual dependence of the two parameters on g_s. Thus, it appeared that variation in ϕ_v mostly served to dampen what would have been the full effect of variation in c_i/c_a on $D_g \cdot TE_c$. For example, plants with low g_s tended to have low c_i/c_a (Fig. 6), which would increase $D_g \cdot TE_c$, as shown in Equation 5. All else being equal, the low g_s would also cause leaf temperature to increase, thereby increasing ϕ_v, which would then cause a counteracting

Table VII. *The C and O isotope composition of experimental plants*

Whole-plant $\delta^{13}C$ values were calculated by weighting the $\delta^{13}C$ for each tissue by the fraction of C in that tissue relative to the whole plant. The $\delta^{13}C$ of stems plus roots was calculated similarly to show the difference between the $\delta^{13}C$ of leaves and heterotrophic tissues. Values are given as the mean for each species, with the SD in parentheses. No SD is given for *P. guatemalensis* because only one individual of this species survived. Sample sizes for the other species ranged from five to eight individuals, as shown in Table III. NA, Not applicable.

Species	Carbon-Isotope Ratio ($\delta^{13}C$) ‰					Oxygen-Isotope Ratio ($\delta^{18}O$) ‰
	Leaves	Stems	Roots	Whole Plant	Leaves − (Stems + Roots)	Stems
Gymnosperm tree species						
C. lusitanica	−29.7 (0.3)	−27.8 (0.4)	−26.8 (1.0)	−28.5 (0.5)	−2.4 (0.5)	20.1 (0.4)
P. caribaea	−30.7 (0.6)	−30.0 (0.6)	−29.4 (0.4)	−30.2 (0.5)	−0.9 (0.2)	20.0 (0.3)
P. guatemalensis	−25.4 (NA)	−23.3 (NA)	−23.5 (NA)	−24.5 (NA)	−2.0 (NA)	24.7 (NA)
T. occidentalis	−28.9 (0.2)	−27.5 (0.3)	−27.2 (0.6)	−28.0 (0.3)	−1.6 (0.5)	20.7 (0.4)
Angiosperm tree species						
C. longifolium	−28.4 (1.3)	−27.2 (0.8)	−28.1 (1.2)	−28.0 (1.1)	−0.7 (0.5)	23.8 (0.6)
C. pratensis	−27.1 (0.3)	−26.4 (0.4)	−26.9 (0.3)	−26.9 (0.3)	−0.4 (0.1)	23.0 (0.3)
H. alchorneoides	−31.0 (0.1)	−29.8 (0.3)	−28.7 (0.4)	−29.6 (0.3)	−2.0 (0.3)	20.6 (0.3)
L. seemannii	−29.3 (0.4)	−28.1 (0.8)	−28.2 (0.4)	−28.6 (0.4)	−1.1 (0.3)	22.8 (0.2)
P. pinnatum	−27.3 (1.1)	−25.7 (1.6)	−25.4 (2.0)	−26.3 (1.3)	−1.7 (0.8)	24.8 (1.3)
S. macrophylla	−31.6 (0.4)	−29.3 (0.3)	−29.1 (0.4)	−30.3 (0.4)	−2.4 (0.1)	23.9 (0.5)
T. rosea	−29.6 (0.8)	−28.0 (0.6)	−27.5 (0.8)	−28.1 (0.7)	−2.0 (0.5)	23.2 (0.3)
T. grandis	−29.5 (0.5)	−28.0 (0.5)	−27.9 (0.6)	−28.6 (0.6)	−1.5 (0.2)	22.9 (0.3)
Angiosperm liana species						
G. lupuloides	−29.2 (0.5)	−28.0 (0.5)	−28.3 (0.3)	−28.4 (0.4)	−1.1 (0.5)	24.8 (0.4)
M. leiostachya	−29.3 (1.3)	−28.0 (1.1)	−27.0 (1.3)	−28.3 (1.3)	−1.7 (0.2)	23.8 (1.0)
S. hypargyreum	−29.5 (0.7)	−29.2 (0.4)	−28.7 (0.5)	−28.9 (0.5)	−0.7 (0.3)	22.4 (1.1)

decrease in $D_g{\cdot}TE_c$. However, it is clear from the large variation in $D_g{\cdot}TE_c$ and its correlation with c_i/c_a (Table VI) that variation in ϕ_v only dampened, and did not completely cancel, the effect of c_i/c_a on $D_g{\cdot}TE_c$. Of the other terms in Equation 5, we found that ϕ_w, the unproductive water loss as a proportion of that associated with photosynthesis, played only a minor role in modulating $D_g{\cdot}TE_c$, in agreement with previous results (Cernusak et al., 2007b). Finally we consider variation in $1 - \phi_c$: although this term is an important functional trait, and may play an important role in modulating *r*, it likely plays a lesser role in controlling $D_g{\cdot}TE_c$ than c_i/c_a. For example if ϕ_c varied among species from 0.3 to 0.5 (Poorter et al., 1990), the term $1 - \phi_c$ would vary from 0.5 to 0.7, whereas we observed variation in $1 - c_i/c_a$ from 0.12 to 0.27 (Table V). Thus, the former would be associated with a 1.4-fold variation in $D_g{\cdot}TE_c$, and the latter with a 2.3-fold variation in $D_g{\cdot}TE_c$.

There was significant variation in $D_g{\cdot}TE_c$ among the plant functional groups that we studied, such that angiosperm trees had highest $D_g{\cdot}TE_c$, on average, and gymnosperm trees lowest, with angiosperm lianas intermediate between the two. Angiosperm trees also had an advantage over gymnosperm trees if water-use efficiency was analyzed as TE_c, $v_g{\cdot}TE_c$, c_i/c_a, or $\Delta^{13}C_p$. Thus, in addition to having an advantage over gymnosperm seedlings in NUE, angiosperm seedlings may also have a competitive advantage in terms of water-use efficiency, when grown in tropical environments. However, it should be emphasized that our experiment was carried out under well-watered conditions, and thus may not necessarily be indicative of trends when water availability is limiting to plant growth.

Of the gymnosperm species that we grew, only one, *Podocarpus guatemalensis*, occurs naturally in the tropical forests of Panama. Although generally associated with highland forests, this species also occurs on lowlying islands off both the Pacific and Atlantic coasts. Unfortunately, only one individual of *P. guatemalensis* survived in our experiment, and we therefore ex-

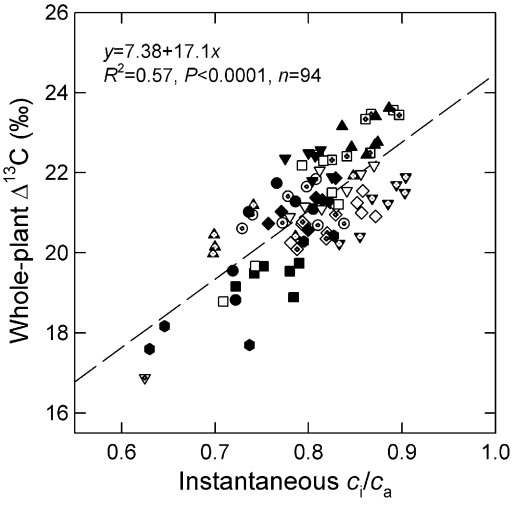

Figure 7. Whole-plant ^{13}C discrimination plotted against the ratio of intercellular to ambient CO_2 partial pressures determined from instantaneous gas exchange measurements. Different symbols refer to different species, as defined in Figure 2.

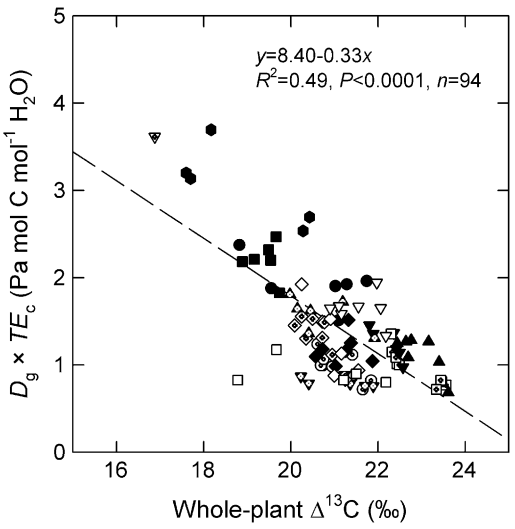

Figure 8. The product of transpiration efficiency of C gain (TE_c) and daytime vapor-pressure deficit of ambient air (D_g) plotted against whole-plant ^{13}C discrimination. Different symbols refer to different species, as defined in Figure 2. Daytime air vapor-pressure deficit was weighted according to the predicted weekly growth increment for each individual plant.

cluded it from all species-level analyses. However, the lone surviving individual was interesting in that it had the highest $D_g \cdot TE_c$ and lowest c_i/c_a of any plant in the study (Figs. 7 and 8). The c_i/c_a of 0.63 that we observed for this individual of *P. guatemalensis* is similar to a c_i/c_a of about 0.60 observed previously for well-watered *Podocarpus lawrencii* (Brodribb, 1996). Further research is necessary to determine whether high water-use efficiency is a common trait within the genus *Podocarpus*, and whether this trait contributes to the ability of *Podocarpus* to persist in otherwise angiosperm-dominated tropical forests.

Stable Isotope Composition

Whole-plant ^{13}C discrimination, $\Delta^{13}C_p$, showed a strong correlation with instantaneous measurements of c_i/c_a (Fig. 7), suggesting that in general $\Delta^{13}C_p$ was a faithful recorder of c_i/c_a, as predicted by Equation 6. The mean value for d that we estimated for the full data set was 3.1‰, reasonably similar to a value of 4.0‰, recently estimated for *Ficus insipida* (Cernusak et al., 2007b). The $\Delta^{13}C_p$ was also a reasonably good predictor of variation in TE_c, $D_g \cdot TE_c$, and $v_g \cdot TE_c$ (Table VI). We previously observed that the relationship between $\Delta^{13}C_p$ and TE_c broke down at the species level, appearing to reflect species-specific offsets in the relationship between the two parameters (Cernusak et al., 2007a). Whereas there was some evidence of similar behavior in this study, as can be seen in Figure 8, the species-level relationship between $\Delta^{13}C_p$ and $D_g \cdot TE_c$ was generally much stronger in this study. For example, in a least-squares linear regression between $\Delta^{13}C_p$ and $D_g \cdot TE_c$ using species means, the former explained 57% of variation in the latter ($R^2 = 0.57$, $P = 0.002$, $n = 14$); if *P. guatemalensis* was included in the regression, the $\Delta^{13}C_p$ explained 77% of variation in $D_g \cdot TE_c$ ($R^2 = 0.77$, $P < 0.0001$, $n = 15$). The main difference between the earlier study (Cernusak et al., 2007a) and this study was likely the range of variation in $\Delta^{13}C_p$ exhibited by the particular species that comprised the experiments. In the earlier study, mean values for $\Delta^{13}C_p$ at the species level ranged from only 20.3 to 21.7‰, whereas in this study, species means ranged from 18.8‰ to 22.9‰; including the individual of *P. guatemalensis* would further extend the lower range to 16.9‰.

Although our results show a generally strong correlation between $\Delta^{13}C_p$ and $D_g \cdot TE_c$, we suggest that it is best to err on the side of caution when interpreting variation among species in the former as indicative of variation among species in the latter. As shown in Equation 7, there are many terms with potential to influence the relationship between $\Delta^{13}C_p$ and $D_g \cdot TE_c$, not the least of which is variation in d, which could be associated with variation among species in mesophyll conductance to CO_2 (Lloyd et al., 1992; Warren and Adams, 2006; Seibt et al., 2008). Moreover, as was previously the case (Cernusak et al., 2007a), we observed significant variation among species in the difference between $\delta^{13}C$ of leaves and that of stems and roots (Table VII). The mechanistic basis for such variation among species in the $\delta^{13}C$ difference between leaves and heterotrophic tissues is not well understood (Hobbie and Werner, 2004; Badeck et al., 2005).

The ^{18}O enrichment of stem dry matter, $\Delta^{18}O_p$, varied significantly among species, and much of the observed variation in $\Delta^{18}O_p$ could be explained by variation in $\Delta^{18}O_e$, the predicted ^{18}O enrichment of evap-

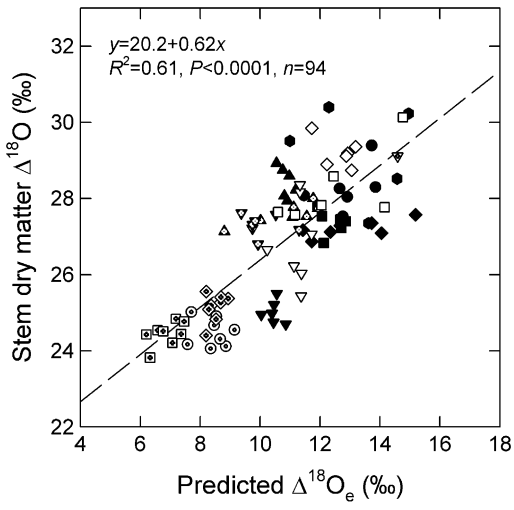

Figure 9. The ^{18}O enrichment of stem dry matter relative to irrigation water plotted against the predicted ^{18}O enrichment of water at the evaporative sites in leaves. The predicted $\Delta^{18}O_e$ was weighted according to the predicted weekly growth increment for each individual plant. Different symbols refer to different species, as defined in Figure 2.

orative sites within leaves (Fig. 9). Because plants were grown over different time periods throughout the year, and due to predicted differences in leaf temperature, there was a reasonable variation among species in predicted $\Delta^{18}O_e$. Species means for growth-weighted $\Delta^{18}O_e$ ranged from 6.9‰ to 13.0‰ (14.6‰ for *P. guatemalensis*), and explained 73% of variation in the observed species means for $\Delta^{18}O_p$ ($R^2 = 0.73$, $P = 0.0001$, $n = 14$), or 75% if *P. guatemalensis* was included ($R^2 = 0.75$, $P < 0.0001$, $n = 15$). These correlations suggest that the assumptions described in the theory section for the $\Delta^{18}O_p$ model are reasonable. Additionally, we observed that the term $1 - [(\Delta^{18}O_p - \varepsilon_{wc} - \varepsilon_{cp})/(1 - p_{ex}p_x)]/\Delta^{18}O_e$ was significantly related to the daytime MTR across the full data set, providing evidence for a Péclet effect, as articulated in Equation 12. This result is consistent with an experiment involving three temperate tree species (Barbour et al., 2004). In this study, we estimated a mean scaled effective path length, L, for the full data set of 53 mm, similar to a value of 54 mm estimated previously for *Eucalyptus globulus* (Cernusak et al., 2005). Analysis of $\Delta^{18}O_p$ in stem dry matter likely provides an advantage over analysis of leaf dry matter for data sets such as ours, which comprise diverse sets of species, because ε_{cp} for stem dry matter tends to be less variable within and among species than ε_{cp} for leaf dry matter (Borella et al., 1999; Barbour et al., 2001; Cernusak et al., 2004, 2005).

Given a sound theoretical understanding of sources of variation in $\delta^{13}C$ and $\delta^{18}O$ in plant dry matter, it should be possible to use such isotopic data to constrain physiological models of tropical forest trees. Data from the present experiment support the suggestion that measurements of $\delta^{13}C$ can be used to make time-integrated estimates of c_i/c_a at the tree or stand scale. The photosynthetic rate, A, can then be predicted from c_i, assuming c_a is known or can be predicted. Finally, g_s can be calculated from A, c_i, and c_a. An example of this modeling approach was recently provided (Buckley, 2008), along with a discussion of its advantages and disadvantages. In the case of $\delta^{18}O$, it should be possible to use this signal to reconstruct the ratio of ambient to intercellular vapor pressures, e_a/e_i, during photosynthesis (Farquhar et al., 1989b; Sternberg et al., 1989). The strong relationship that we observed between stem dry matter $\Delta^{18}O_p$ and the predicted $\Delta^{18}O_e$ (Fig. 9) supports this idea. However, our analysis also confirmed that the relationship between $\Delta^{18}O_p$ and $\Delta^{18}O_e$ was further modified by transpiration rate, E, suggesting that it may be necessary to obtain information independently about E to calculate e_a/e_i from $\Delta^{18}O_p$. Such information might be obtained from sap flux measurements or eddy covariance data, for example. Assuming e_a is known or can be predicted, an estimate of e_i based on $\Delta^{18}O_p$ might then be particularly valuable, as it was recently suggested that the leaf-to-air vapor pressure difference, e_i-e_a, will likely be an important control over productivity in tropical forest trees in the face of changing climate (Lloyd and Farquhar, 2008).

CONCLUSION

We observed that $1/\rho$ was an important control over relative growth rate, r, in a diverse group of seedlings grown under tropical field conditions, including gymnosperm trees, angiosperm trees, and angiosperm lianas. The gymnosperm trees generally had lower $1/\rho$ and r than the angiosperm species, and this may have reflected differences in the hydraulic efficiency of plant biomass among functional groups. Additionally, we observed that A_n, the photosynthetic NUE, was the primary control over whole-plant NUE, and that the gymnosperm species appeared to be at a significant disadvantage with respect to this trait compared to angiosperm species. Variation in whole-plant water use efficiency among species was primarily controlled by c_i/c_a, which in turn varied as a function of stomatal conductance. Whole-plant ^{13}C discrimination was also controlled by c_i/c_a, and thus correlated with whole-plant water use efficiency. The ^{18}O enrichment of stem dry matter of the experimental plants varied primarily as a function of the predicted ^{18}O enrichment of evaporative site water within leaves, and secondarily as a function of the daytime MTR. Results provided quantitative information about the mechanisms controlling fluxes of C and water between forest trees and the atmosphere, and the coupling of these processes to plant N status. Moreover, our data set enabled rigorous testing of the theoretical basis for variation in ^{13}C and ^{18}O of plant dry matter; measurements of these stable isotope ratios could prove useful for parameterizing forest ecosystem process models.

MATERIALS AND METHODS

Study Site and Plant Material

The study was carried out at the Santa Cruz Experimental Field Facility, a part of the Smithsonian Tropical Research Institute, located in Gamboa, Republic of Panama (9°07′ N, 79°42′ W), at an altitude of approximately 28 m above sea level. Average meteorological conditions at the study site during the experiment are shown in Table II. These values were calculated from data collected on site every 15 min by an automated weather station (Winter et al., 2001, 2005). Seedlings of *Cupressus lusitanica*, *Pinus caribaea*, and *Thuja occidentalis* were obtained from a commercial nursery in Chiriqui Province, Republic of Panama. All other species were grown from seed collected in the Panama Canal watershed, or obtained as seedlings from PRORENA, a native species reforestation initiative operated through the Center for Tropical Forest Science at the Smithsonian Tropical Research Institute. Familial associations for each species are shown in Table III. The species *C. lusitanica* and *P. caribaea* are conifers, with native distributions extending from Mexico to Nicaragua. *T. occidentalis* is a conifer native to northeastern North America, and *Tectona grandis* is a timber species native to south and southeast Asia. All other species included in the study occur naturally in Panama.

The initial dry mass at the commencement of transpiration measurements for each species is shown in Table III; these dry masses were estimated by harvesting three to five individuals judged to be similar in size to the seedlings retained for the experiment. Seedlings were transplanted individually into 38-L plastic pots (Rubbermaid Round Brute; Consolidated). Each pot contained 25 kg of dry soil mixture, which comprised 60% by volume dark, air-dried top soil, and 40% by volume air-dried rice (*Oryza sativa*) husks. The rice husks were added to improve soil structure and drainage. The pot water content was brought to field capacity by the addition of 8 kg of water. The soil surface was covered with 2 kg of gravel to minimize soil evaporation, and the outer walls of each pot were lined with reflective insulation to minimize heating by

sunlight. A metal trellis was added to each pot containing a liana seedling. The pots were situated under a rain shelter with a glass roof, such that there was essentially no interception of rain by the pots in the otherwise open-air conditions. The initiation of measurements varied among species, due to the temporal variation in the availability of seed and seedlings. Harvest dates also varied, depending on the date of initiation of measurements and growth rates; there were three harvests in total. The start and end dates of transpiration measurements for each species are given in Table III.

Growth and Transpiration Efficiency Measurements

Pots were weighed at a minimum frequency of once per week to the nearest 5 g with a 64-kg capacity balance (Sartorius QS64B; Thomas). After the mass was recorded, water was added to each pot to restore it to its mass at field capacity. As plant water use increased with increasing plant size, the pots were weighed and watered more frequently. We endeavored to maintain pot water content above 5 kg at all times, such that the range of soil water contents experienced by the plants ranged approximately from field capacity to 60% of field capacity. Control pots without plants were deployed among the pots with plants in a ratio of one control pot to each six planted pots. The control pots were weighed each week to estimate soil evaporation. Cumulative plant water use was calculated as the sum of pot water loss over the course of the experiment minus the average water loss of control pots for the same time period. Shortly before plant harvest, the pots were weighed at dawn and dusk for 2 d to calculate nighttime transpiration separately from daytime transpiration. Immediately following plant harvest, total plant leaf area was measured with a leaf area meter (LI-3100; LI-COR). Leaves, stems, and roots were separated at harvest and oven-dried to a constant mass at 70°C; they were then weighed to the nearest 0.02 g.

The mean relative growth rate, r, of each plant was calculated as $r = [\ln(m_{c2}) - \ln(m_{c1})]/t$, where $\ln(m_{c2})$ and $\ln(m_{c1})$ are natural logarithms of the C mass at the end and beginning of the experiment, respectively, and t is the duration of the experiment (Blackman, 1919). The MTR over the course of the experiment was calculated as the cumulative water transpired divided by the leaf area duration (Sheshshayee et al., 2005): $\text{MTR} = E_t/[(\text{LA}_1 + \text{LA}_2)0.5t]$, where E_t is cumulative water transpired, and LA_1 and LA_2 are the leaf area at the beginning and end of the experiment, respectively. The transpiration efficiency of C gain, TE_c, was calculated as $\text{TE}_c = (m_{c2} - m_{c1} + l_c)/E_t$, where l_c is the C mass of leaf litter abscised during the experiment.

To compare the D experienced by species that were grown over different time periods (Table III), we calculated a growth-weighted D for each individual plant. Dry matter increments were predicted at weekly time steps for each plant using relative growth rates calculated over the full experiment. Thus, the dry matter increment for week 1, w_1, was calculated as $w_1 = m_1 - m_0$, where m_0 was initial plant dry mass, and m_1 was calculated as $m_1 = m_0 e^{rt}$, with $t = 7$ d; the r was calculated as described above. The dry matter increment in week 2, w_2, was then calculated as $w_2 = m_2 - m_1$, where m_2 was calculated as $m_2 = m_1 e^{rt}$, with t again set at 7 d, and so on. For each week during the experimental period, we also calculated an average daytime D from the meteorological data collected at 15-min intervals. Growth-weighted D, D_g, was then calculated as

$$D_g = \frac{\sum_{i=1}^{n} D_i w_i}{\sum_{i=1}^{n} w_i} \quad (13)$$

where D_i is the average daytime D for week i (kPa), and w_i is the predicted dry matter increment for week i (g).

In addition to calculating a growth-weighted D for each species, we also predicted a growth-weighted v. Average weekly v for each plant was predicted using a leaf energy balance model developed by D.G.G. dePury and G.D. Farquhar (unpublished data), and described by Barbour et al. (2000a). The model was parameterized with weekly average daytime values for air temperature, relative humidity, irradiance, and wind speed taken from the data collected by the automated weather station. Stomatal conductance for each plant, measured as described below, was further used to parameterize the model. The model predicted average weekly daytime leaf temperature for each plant. The intercellular water vapor pressure, e_i, was then calculated as the saturation vapor pressure at leaf temperature, and this value was used to calculate an average weekly value of v for each plant. The growth-weighted v, v_g, was then calculated as in Equation 13, but replacing D_i with v_i, the average daytime v for week i.

In a similar fashion, we predicted a growth-weighted $\Delta^{18}O_e$ for each plant. For each weekly time step, the predicted value of e_a/e_i was used with Equation 8 to calculate average weekly daytime $\Delta^{18}O_e$. The $\Delta^{18}O_v$ was assumed equal to $-\varepsilon^+$, calculated from air temperature (Bottinga and Craig, 1969). Growth-weighted $\Delta^{18}O_e$, $\Delta^{18}O_{eg}$, was then calculated for each plant as in Equation 13, but replacing D_i with $\Delta^{18}O_{ei}$, the average daytime $\Delta^{18}O_e$ for week i.

Leaf Gas Exchange and Leaf Temperature Measurements

We measured leaf gas exchange on three to five leaves per plant in the week preceding plant harvest with a Li-6400 portable photosynthesis system (LI-COR). Leaves were illuminated with an artificial light source (6400-02B LED; LI-COR) at a photon flux density of 1,200 μmol m^{-2} s^{-1}. Measurements were made during both the morning and afternoon for each plant, and the mean of the two sets of measurements was taken for each individual. The mean leaf temperature during measurements was 32.7 ± 1.5°C (mean ± 1 SD), and the mean v was 1.55 ± 0.46 kPa (mean ± 1 SD).

Several days prior to the harvests that took place on March 11, 2006 and May 10, 2006 (Table III), we made measurements of leaf temperature with a hand-held infrared thermometer (Raytek MT Minitemp; Forestry Suppliers). Measurements were repeated two to three times on three to five leaves per plant under clear-sky conditions near midday. Values for each plant were averaged, and v was calculated from measurements of relative humidity and air temperature, assuming e_i was at saturation at the average leaf temperature for each plant. Leaf temperature was not measured for the plants harvested on December 13, 2005 (Table III).

Stable Isotope and Elemental Analyses

Leaf, stem, and root dry matter were ground to a fine, homogeneous powder for analysis of isotopic and elemental composition. The $\delta^{13}C$, total C, and total N concentrations were determined on subsamples of approximately 3 mg, combusted in an elemental analyzer (ECS 4010; Costech Analytical Technologies) coupled to a continuous flow isotope ratio mass spectrometer (Delta XP; Finnigan MAT). The $\delta^{18}O$ of stem dry matter was determined on subsamples of approximately 1 mg (Delta XP; Finnigan MAT), following pyrolysis in a high-temperature furnace (Thermoquest TC/EA; Finnigan MAT). Analyses were carried out at the Stable Isotope Core Laboratory, Washington State University. The $\delta^{13}C$ and $\delta^{18}O$ values were expressed in δ notation with respect to the standards of PeeDee Belemnite and Vienna Standard Mean Ocean Water, respectively. The ^{13}C discrimination of plant dry matter ($\Delta^{13}C_p$) was calculated as $\Delta^{13}C_p = (\delta^{13}C_a - \delta^{13}C_p)/(1 + \delta^{13}C_p)$, where $\delta^{13}C_a$ is the $\delta^{13}C$ of CO_2 in air and $\delta^{13}C_p$ is that of plant dry matter. We assumed a $\delta^{13}C_a$ of −8‰. The oxygen isotope enrichment of stem dry matter ($\Delta^{18}O_p$) was calculated as $\Delta^{18}O_p = (\delta^{18}O_p - \delta^{18}O_s)/(1 + \delta^{18}O_s)$, where $\delta^{18}O_p$ is $\delta^{18}O$ of stem dry matter, and $\delta^{18}O_s$ is that of irrigation (source) water. Irrigation water was drawn from two 800-L tanks, sealed to prevent evaporation, which were periodically refilled with tap water, to buffer against short-term variation in $\delta^{18}O_s$. The tank water had a mean $\delta^{18}O$ of −4.3 ± 0.5‰ (mean ± 1 SD, $n = 6$); we therefore calculated $\Delta^{18}O_p$ assuming a $\delta^{18}O_s$ of −4.3‰.

Leaf dry matter was further analyzed for P, K, and Ca concentrations by acid digestion and detection on an inductively coupled plasma optical-emission spectrometer (Perkin Elmer). Leaf samples were prepared by digesting approximately 200 mg of sample material under pressure in polytetrafluoroethylene vessels with 2 mL of concentrated nitric acid.

Statistical Analyses

We analyzed relationships between continuous variables using least-squares linear regression. Variation among species and among functional groups (gymnosperm trees, angiosperm trees, and angiosperm lianas) was assessed with a nested design in the general linear model routine of SYSTAT 11 (SYSTAT Software); the functional group and species nested within the functional group were taken as independent factors. For these analyses, the number of observations was 93, the degrees of freedom for the functional group was 2, the degrees of freedom for species nested within the functional group was 11, and the degrees of freedom error was 79. Pairwise comparisons among species or functional groups were then carried out according to Tukey's method. Among the study species, there was one, *Podocarpus guatemalensis*, for which only one individual survived. All other species

comprised between five and eight individuals, as shown in Table III. Because there was only one individual of *P. guatemalensis*, we excluded this species from analyses aimed at assessing variation among functional groups and species. However, we included the individual in linear regression analyses of continuous variables. We considered it important to report data for this individual, as it represents the only gymnosperm species in the study native to the tropical forests of Panama.

Supplemental Data

The following materials are available in the on-line version of this article.

Supplemental Table S1. The C and N concentrations of experimental plants.

ACKNOWLEDGMENTS

We thank Milton Garcia and Aurelio Virgo for technical assistance, and Ben Harlow for carrying out isotopic and elemental analyses.

Received May 26, 2008; accepted June 23, 2008; published July 3, 2008.

LITERATURE CITED

Aerts R, Chapin FS (2000) The mineral nutrition of wild plants revisited: a re-evaluation of processes and patterns. Adv Ecol Res **30:** 1–67

Atkin OK, Schortemeyer M, McFarlane N, Evans JR (1998) Variation in the components of relative growth rate in ten *Acacia* species from contrasting environments. Plant Cell Environ **21:** 1007–1017

Badeck FW, Tcherkez G, Nogues S, Piel C, Ghashghaie J (2005) Post-photosynthetic fractionation of stable carbon isotopes between plant organs—a widespread phenomenon. Rapid Commun Mass Spectrom **19:** 1381–1391

Barbour MM (2007) Stable oxygen isotope composition of plant tissue: a review. Funct Plant Biol **34:** 83–94

Barbour MM, Andrews JT, Farquhar GD (2001) Correlations between oxygen isotope ratios of wood constituents of *Quercus* and *Pinus* samples from around the world. Aust J Plant Physiol **28:** 335–348

Barbour MM, Farquhar GD (2000) Relative humidity- and ABA-induced variation in carbon and oxygen isotope ratios of cotton leaves. Plant Cell Environ **23:** 473–485

Barbour MM, Farquhar GD (2004) Do pathways of water movement and leaf anatomical dimensions allow development of gradients in $H_2{}^{18}O$ between veins and the sites of evaporation within leaves? Plant Cell Environ **27:** 107–121

Barbour MM, Fischer RA, Sayre KD, Farquhar GD (2000a) Oxygen isotope ratio of leaf and grain material correlates with stomatal conductance and grain yield in irrigated wheat. Aust J Plant Physiol **27:** 625–637

Barbour MM, Roden JS, Farquhar GD, Ehleringer JR (2004) Expressing leaf water and cellulose oxygen isotope ratios as enrichment above source water reveals evidence of a Péclet effect. Oecologia **138:** 426–435

Barbour MM, Schurr U, Henry BK, Wong SC, Farquhar GD (2000b) Variation in the oxygen isotope ratio of phloem sap sucrose from castor bean. Evidence in support of the Péclet effect. Plant Physiol **123:** 671–679

Blackman VH (1919) The compound interest law and plant growth. Ann Bot (Lond) **33:** 353–360

Bond WJ (1989) The tortoise and the hare: ecology of angiosperm dominance and gymnosperm persistence. Biol J Linn Soc **36:** 227–249

Borella S, Leuenberger M, Saurer M (1999) Analysis of $\delta^{18}O$ in tree rings: wood-cellulose comparison and method dependent sensitivity. J Geophys Res **104:** 19,267–19,273

Bottinga Y, Craig H (1969) Oxygen isotope fractionation between CO_2 and water, and the isotopic composition of marine atmospheric CO_2. Earth Planet Sci Lett **5:** 285–295

Brodribb T (1996) Dynamics of changing intercellular CO_2 concentration (c_i) during drought and determination of minimum functional c_i. Plant Physiol **111:** 179–185

Brodribb TJ, Holbrook NM, Hill RS (2005) Seedling growth in conifers and angiosperms: impacts of contrasting xylem structure. Aust J Bot **53:** 749–755

Buckley TN (2008) The role of stomatal acclimation in modelling tree adaptation to high CO_2. J Exp Bot **59:** 1951–1961

Cappa CD, Hendricks MB, DePaulo DJ, Cohen RC (2003) Isotopic fractionation of water during evaporation. J Geophys Res **108:** 4525

Cernusak LA, Aranda J, Marshall JD, Winter K (2007a) Large variation in whole-plant water-use efficiency among tropical tree species. New Phytol **173:** 294–305

Cernusak LA, Farquhar GD, Pate J (2005) Environmental and physiological controls over oxygen and carbon isotope composition of Tasmanian blue gum, *Eucalyptus globulus*. Tree Physiol **25:** 129–146

Cernusak LA, Pate JS, Farquhar GD (2004) Oxygen and carbon isotope composition of parasitic plants and their hosts in southwestern Australia. Oecologia **139:** 199–213

Cernusak LA, Winter K, Aranda J, Turner BL, Marshall JD (2007b) Transpiration efficiency of a tropical pioneer tree (*Ficus insipida*) in relation to soil fertility. J Exp Bot **58:** 3549–3566

Cernusak LA, Wong SC, Farquhar GD (2003) Oxygen isotope composition of phloem sap in relation to leaf water in *Ricinus communis*. Funct Plant Biol **30:** 1059–1070

Cornelissen JHC, Diez PC, Hunt R (1996) Seedling growth, allocation and leaf attributes in a wide range of woody plant species and types. J Ecol **84:** 755–765

Craig H, Gordon LI (1965) Deuterium and oxygen-18 variations in the ocean and the marine atmosphere. *In* E Tongiorgi, ed, Proceedings of a Conference on Stable Isotopes in Oceanographic Studies and Palaeotemperatures. Lischi and Figli, Pisa, Italy, pp 9–130

Cuntz M, Ogée J, Farquhar GD, Peylin P, Cernusak LA (2007) Modelling advection and diffusion of water isotopologues in leaves. Plant Cell Environ **30:** 892–909

Dongmann G, Nurnberg HW, Förstel H, Wagener K (1974) On the enrichment of $H_2{}^{18}O$ in the leaves of transpiring plants. Radiat Environ Biophys **11:** 41–52

Evans GC (1972) The quantitative analysis of plant growth. Blackwell Scientific, Oxford

Farquhar GD, Cernusak LA, Barnes B (2007) Heavy water fractionation during transpiration. Plant Physiol **143:** 11–18

Farquhar GD, Condon AG, Masle J (1994) Use of carbon and oxygen isotope composition and mineral ash content in breeding for improved rice production under favorable, irrigated conditions. *In* KG Cassman, ed, Breaking the Yield Barrier. International Rice Research Institute, Manila, Philippines, pp 95–101

Farquhar GD, Ehleringer JR, Hubick KT (1989a) Carbon isotope discrimination and photosynthesis. Annu Rev Plant Physiol Plant Mol Biol **40:** 503–537

Farquhar GD, Gan KS (2003) On the progressive enrichment of the oxygen isotopic composition of water along leaves. Plant Cell Environ **26:** 801–819

Farquhar GD, Hubick KT, Condon AG, Richards RA (1989b) Carbon isotope fractionation and plant water-use efficiency. *In* PW Rundel, JR Ehleringer, KA Nagy, eds, Stable Isotopes in Ecological Research, Springer-Verlag, New York, pp 21–46

Farquhar GD, Lloyd J (1993) Carbon and oxygen isotope effects in the exchange of carbon dioxide between terrestrial plants and the atmosphere. *In* JR Ehleringer, AE Hall, GD Farquhar, eds, Stable Isotopes and Plant Carbon-Water Relations. Academic Press, San Diego, pp 47–70

Farquhar GD, O'Leary MH, Berry JA (1982) On the relationship between carbon isotope discrimination and the intercellular carbon dioxide concentration in leaves. Aust J Plant Physiol **9:** 121–137

Farquhar GD, Richards RA (1984) Isotopic composition of plant carbon correlates with water-use efficiency in wheat genotypes. Aust J Plant Physiol **11:** 539–552

Flanagan LB (1993) Environmental and biological influences on the stable oxygen and hydrogen isotopic composition of leaf water. *In* JR Ehleringer, AE Hall, GD Farquhar, eds, Stable Isotopes and Plant Carbon-Water Relations. Academic Press, San Diego, pp 71–89

Flanagan LB, Phillips SL, Ehleringer JR, Lloyd J, Farquhar GD (1994) Effect of changes in leaf water oxygen isotopic composition on discrimination against $C^{18}O^{16}O$ during photosynthetic gas exchange. Aust J Plant Physiol **21:** 221–234

Gartner BL, Bullock SH, Mooney HA, Brown VB, Whitbeck JL (1990) Water transport properties of vine and tree stems in tropical deciduous forest. Am J Bot **77:** 742–749

Gessler A, Peuke AD, Keitel C, Farquhar GD (2007) Oxygen isotope

enrichment of organic matter in *Ricinus communis* during the diel course and as affected by assimilate transport. New Phytol **174:** 600–613

Hobbie EA, Werner RA (2004) Intramolecular, compound-specific, and bulk carbon isotope patterns in C_3 and C_4 plants: a review and synthesis. New Phytol **161:** 371–385

Hubick KT, Farquhar GD (1989) Carbon isotope discrimination and the ratio of carbon gained to water lost in barley cultivars. Plant Cell Environ **12:** 795–804

Hubick KT, Farquhar GD, Shorter R (1986) Correlation between water-use efficiency and carbon isotope discrimination in diverse peanut (*Arachis*) germplasm. Aust J Plant Physiol **13:** 803–816

Kahmen A, Simonin K, Tu KP, Merchant A, Callister A, Siegwolf R, Dawson TE, Arndt SK (2008) Effects of environmental parameters, leaf physiological properties and leaf water relations on leaf water $\delta^{18}O$ enrichment in different *Eucalyptus* species. Plant Cell Environ **31:** 738–751

Koerselman W, Meuleman AFM (1996) The vegetation N:P ratio: a new tool to detect the nature of nutrient limitation. J Appl Ecol **33:** 1441–1450

Laurance WF, Oliveira AA, Laurance SG, Condit R, Nascimento HEM, Sanchez-Thorin AC, Lovejoy TE, Andrade A, D'Angelo S, Ribeiro JE, et al (2004) Pervasive alteration of tree communities in undisturbed Amazonian forests. Nature **428:** 171–175

LeBauer DS, Treseder KK (2008) Nitrogen limitation of net primary productivity in terrestrial ecosystems is globally distributed. Ecology **89:** 371–379

Lloyd J, Farquhar GD (2008) Effects of rising temperatures and $[CO_2]$ on the physiology of tropical forest trees. Philos Trans R Soc Lond B Biol Sci **363:** 1811–1817

Lloyd J, Syvertsen JP, Kriedemann PE, Farquhar GD (1992) Low conductances for CO_2 diffusion from stomata to the sites of carboxylation in leaves of woody species. Plant Cell Environ **15:** 873–899

Long SP, Farage PK, Garcia RL (1996) Measurement of leaf and canopy photosynthetic CO_2 exchange in the field. J Exp Bot **47:** 1629–1642

Masle J, Farquhar GD (1988) Effects of soil strength on the relation of water-use efficiency and growth to carbon isotope discrimination in wheat seedlings. Plant Physiol **86:** 32–38

Poorter H (1994) Construction costs and payback time of biomass: a whole plant perspective. *In* J Roy, E Garnier, eds, A Whole Plant Perspective on Carbon-Nitrogen Interactions. SPB Academic Publishing, The Hague, The Netherlands, pp 11–127

Poorter H, Remkes C (1990) Leaf-area ratio and net assimilation rate of 24 wild species differing in relative growth rate. Oecologia **83:** 553–559

Poorter H, Remkes C, Lambers H (1990) Carbon and nitrogen economy of 24 wild species differing in relative growth rate. Plant Physiol **94:** 621–627

Reich PB, Oleksyn J (2004) Global patterns of plant leaf N and P in relation to temperature and latitude. Proc Natl Acad Sci USA **101:** 11001–11006

Ripullone F, Matsuo N, Stuart-Williams H, Wong SC, Borghetti M, Tani M, Farquhar GD (2008) Environmental effects on oxygen isotope enrichment of leaf water in cotton leaves. Plant Physiol **146:** 729–736

Roden JS, Lin GG, Ehleringer JR (2000) A mechanistic model for interpretation of hydrogen and oxygen isotope ratios in tree-ring cellulose. Geochim Cosmochim Acta **64:** 21–35

Seibt U, Rajabi A, Griffiths H, Berry JA (2008) Carbon isotopes and water use efficiency: sense and sensitivity. Oecologia **155:** 441–454

Sheshshayee MS, Bindumadhava H, Ramesh R, Prasad TG, Lakshminarayana MR, Udayakumar M (2005) Oxygen isotope enrichment ($\Delta^{18}O$) as a measure of time-averaged transpiration rate. J Exp Bot **56:** 3033–3039

Sperry JS, Hacke UG, Pittermann J (2006) Size and function in conifer tracheids and angiosperm vessels. Am J Bot **93:** 1490–1500

Sternberg LSL, Mulkey SS, Wright SJ (1989) Oxygen isotope ratio stratification in a tropical moist forest. Oecologia **81:** 51–56

Tanner CB, Sinclair TR (1983) Efficient water use in crop production: research or re-search. *In* H Taylor, ed, Limitations to Efficient Water Use in Crop Production. ASA-CSSA-SSSA, Madison, WI, pp 1–28

Tanner EVJ, Vitousek PM, Cuevas E (1998) Experimental investigation of nutrient limitation of forest growth on wet tropical mountains. Ecology **79:** 10–22

Vertregt N, Penning de Vries FWT (1987) A rapid method for determining the efficiency of biosynthesis of plant biomass. J Theor Biol **128:** 109–119

Warren CR, Adams MA (2006) Internal conductance does not scale with photosynthetic capacity: implications for carbon isotope discrimination and the economics of water and nitrogen use in photosynthesis. Plant Cell Environ **29:** 192–201

Winter K, Aranda J, Garcia M, Virgo A, Paton SR (2001) Effect of elevated CO_2 and soil fertilization on whole-plant growth and water use in seedlings of a tropical pioneer tree, *Ficus insipida* Willd. Flora **196:** 458–464

Winter K, Aranda J, Holtum JAM (2005) Carbon isotope composition and water-use efficiency in plants with crassulacean acid metabolism. Funct Plant Biol **32:** 381–388

Wright IJ, Westoby M (2000) Cross-species relationships between seedling relative growth rate, nitrogen productivity and root *vs* leaf function in 28 Australian woody species. Funct Ecol **14:** 97–107

Wright SJ (2005) Tropical forests in a changing environment. Trends Ecol Evol **20:** 553–560

Yakir D, DeNiro MJ, Rundel PW (1989) Isotopic inhomogeneity of leaf water: evidence and implications for the use of isotopic signals transduced by plants. Geochim Cosmochim Acta **53:** 2769–2773

Yakir D, Israeli Y (1995) Reduced solar irradiance effects on net primary productivity (NPP) and the $\delta^{13}C$ and $\delta^{18}O$ values in plantations of *Musa* sp. *Musaceae*. Geochim Cosmochim Acta **59:** 2149–2151